Large-scale analysis of structural brain asymmetries in schizophrenia via the ENIGMA consortium

Dick Schijven[1], Merel C. Postema[1,2], Masaki Fukunaga[3], Junya Matsumoto[4], Kenichiro Miura[4], Sonja M.C. de Zwarte[5], Neeltje E.M. van Haren[5,6], Wiepke Cahn[5], Hilleke E. Hulshoff Pol[5], René S. Kahn[5,7,8], Rosa Ayesa-Arriola[9,10,11], Víctor Ortiz-García de la Foz[10,12], Diana Tordesillas-Gutierrez[13,14], Javier Vázquez-Bourgon[9,10], Benedicto Crespo-Facorro[10,15], Dag Alnæs[16,17,18], Andreas Dahl[17], Lars T. Westlye[16,17,19,20], Ingrid Agartz[16,21,22], Ole A. Andreassen[16,19], Erik G. Jönsson[16,22], Peter Kochunov[23], Jason M. Bruggemann[24,25,26,27], Stanley V. Catts[28], Patricia T. Michie[29], Bryan J. Mowry[30,31], Yann Quidé[24,25], Paul E. Rasser[32,33,34], Ulrich Schall[32], Rodney J. Scott[35], Vaughan J. Carr[24,25], Melissa J. Green[24,25], Frans A. Henskens[36,37], Carmel M. Loughland[36,38], Christos Pantelis[39], Cynthia Shannon Weickert[24,25,40], Thomas W. Weickert[24,25,40], Lieuwe de Haan[41,42], Katharina Brosch[43,44], Julia-Katharina Pfarr[43,44], Kai G. Ringwald[43,44], Frederike Stein[43,44], Andreas Jansen[43,44,45], Tilo T.J. Kircher[43,44], Igor Nenadić[43,44], Bernd Krämer[46], Oliver Gruber[46], Theodore D. Satterthwaite[47,48,49], Juan Bustillo[50], Daniel H. Mathalon[51,52], Adrian Preda[53], Vince D. Calhoun[54,55], Judith M. Ford[56], Steven G. Potkin[53,57], Jingxu Chen[58], Yunlong Tan[58], Zhiren Wang[58], Hong Xiang[59], Fengmei Fan[58], Fabio Bernardoni[60,61], Stefan Ehrlich[60,61], Paola Fuentes-Claramonte[62,63], Maria Angeles Garcia-Leon[62,63], Amalia Guerrero-Pedraza[62,64], Raymond Salvador[62,63], Salvador Sarró[62,63], Edith Pomarol-Clotet[62,63], Valentina Ciullo[65], Fabrizio Piras[65], Daniela Vecchio[65], Nerisa Banaj[65], Gianfranco Spalletta[65,66], Stijn Michielse[67], Therese van Amelsvoort[67], Erin W. Dickie[68,69], Aristotle N. Voineskos[68,69], Kang Sim[70,71], Simone Ciufolini[72], Paola Dazzan[73], Robin M. Murray[72], Woo-Sung Kim[74,75], Young-Chul Chung[74,75], Christina Andreou[76,77], André Schmidt[76], Stefan Borgwardt[76,77], Andrew M. McIntosh[78], Heather C. Whalley[78], Stephen M. Lawrie[78], Stefan du Plessis[79,80], Hilmar K. Luckhoff[79], Freda Scheffler[79,81,82], Robin Emsley[79], Dominik Grotegerd[83], Rebekka Lencer[77,83], Udo Dannlowski[83], Jesse T. Edmond[54], Kelly Rootes-Murdy[54], Julia M. Stephen[84], Andrew R. Mayer[84], Linda A. Antonucci[85], Leonardo Fazio[86], Giulio Pergola[86], Alessandro Bertolino[86,87], Covadonga M. Díaz-Caneja[88,89,90,91], Joost Janssen[88,89,90], Noemi G. Lois[88,90], Celso Arango[88,89,90,91], Alexander S. Tomyshev[92], Irina Lebedeva[92], Simon Cervenka[22,93], Carl M. Sellgren[22,94], Foivos Georgiadis[95], Matthias Kirschner[95,96], Stefan Kaiser[95,97], Tomas Hajek[98,99], Antonin Skoch[98,100], Filip Spaniel[98], Minah Kim[101,102], Yoo Bin Kwak[103], Sanghoon Oh[102], Jun Soo Kwon[101,102], Anthony James[104], Geor Bakker[67], Christian Knöchel[105], Michael Stäblein[105], Viola Oertel[105], Anne Uhlmann[81,106], Fleur M. Howells[81,82], Dan J. Stein[81,82,107], Henk S. Temmingh[81], Ana M. Diaz-Zuluaga[108], Julian A. Pineda-Zapata[108], Carlos López-Jaramillo[108], Stephanie Homan[95,109], Ellen Ji[95], Werner Surbeck[95], Philipp Homan[95,110,111,112], Simon E. Fisher[1,113], Barbara Franke[113,114,115], David C. Glahn[116,117], Ruben C. Gur[47,48,118,119], Ryota Hashimoto[4], Neda Jahanshad[120], Eileen Luders[121,122,123], Sarah E. Medland[124], Paul M. Thompson[120], Jessica A. Turner[54,55], Theo G.M. van Erp[125,126], Clyde Francks[1,113,114,*]

1 Language & Genetics Department, Max Planck Institute for Psycholinguistics, Nijmegen, The Netherlands
2 Alzheimer Center Amsterdam, Department of Neurology, Amsterdam Neuroscience, Amsterdam UMC, Vrije Universiteit Amsterdam, Amsterdam, The Netherlands
3 Division of Cerebral Integration, National Institute for Physiological Sciences, Okazaki, Aichi, Japan
4 Department of Pathology of Mental Diseases, National Institute of Mental Health, National Center of Neurology and Psychiatry, Tokyo, Japan
5 Department of Psychiatry, University Medical Center Utrecht Brain Center, University Medical Center Utrecht, Utrecht University, Utrecht, The Netherlands
6 Department of Child and Adolescent Psychiatry/Psychology, Erasmus University Medical Center-Sophia Children's Hospital, Rotterdam, The Netherlands
7 Department of Psychiatry, Icahn School of Medicine at Mount Sinai, New York, NY, USA

8 The Mental Illness Research, Education and Clinical Centers (MIRECC), James J. Peters VA Medical Center, Bronx, New York, NY, USA
9 Department of Psychiatry, University Hospital Marqués de Valdecilla, Instituto de Investigación Marqués de Valdecilla (IDIVAL), Santander, Spain
10 Centro de Investigación Biomédica en Red de Salud Mental (CIBERSAM), Instituto de Salud Carlos III, Madrid, Spain
11 Department of Medicine and Psychiatry, School of Medicine, University of Cantabria, Santander, Spain
12 Department of Psychiatry, Marqués de Valdecilla University Hospital, IDIVAL, School of Medicine, University of Cantabria, Santander, Spain
13 Department of Radiology, Instituto de Investigación Marqués de Valdecilla (IDIVAL), Marqués de Valdecilla University Hospital, Santander, Spain
14 Advanced Computing and e-Science, Instituto de Física de Cantabria (UC-CSIC), Santander, Spain
15 Department of Psychiatry, School of Medicine, University of Sevilla, University Hospital Virgen del Rocío, CSIC - IBiS, Sevilla, Spain
16 Norwegian Centre for Mental Disorders Research (NORMENT), Institute of Clinical Medicine, University of Oslo, Oslo, Norway
17 Department of Psychology, University of Oslo, Oslo, Norway
18 Bjørknes College, Oslo, Norway
19 Division of Mental Health and Addiction, Oslo University Hospital, Oslo, Norway
20 KG Jebsen Center for Neurodevelopmental Disorders, University of Oslo, Oslo, Norway
21 Department of Psychiatric Research, Diakonhjemmet Hospital, Oslo, Norway
22 Centre for Psychiatry Research, Department of Clinical Neuroscience, Karolinska Institutet & Stockholm Health Care Services, Region Stockholm, Stockholm, Sweden
23 Department of Psychiatry, University of Maryland School of Medicine, Baltimore, MD, USA
24 School of Psychiatry, University of New South Wales (UNSW), Sydney, NSW, Australia
25 Neuroscience Research Australia, Randwick, NSW, Australia
26 Edith Collins Centre (Translational Research in Alcohol Drugs & Toxicology), Sydney Local Health District, Sydney, NSW, Australia
27 Specialty of Addiction Medicine, Central Clinical School, Faculty of Medicine and Health, University of Sydney, Sydney, NSW, Australia
28 School of Medicine, University of Queensland, Herston, QLD, Australia
29 School of Psychological Sciences, University of Newcastle, Callaghan, NSW, Australia
30 Queensland Brain Institute, The University of Queensland, Brisbane, QLD, Australia
31 Queensland Centre for Mental Health Research, The University of Queensland, Brisbane, QLD, Australia
32 Centre for Brain and Mental Health Research, University of Newcastle, Callaghan, NSW, Australia
33 Priority Research Centre for Stroke and Brain Injury, University of Newcastle, Callaghan, NSW, Australia
34 Hunter Medical Research Institute (HMRI), New Lambton Heights, NSW, Australia
35 School of Biomedical Science and Pharmacy, Faculty of Health and Medicine, University of Newcastle, Callaghan, NSW, Australia
36 School of Medicine and Public Health, University of Newcastle, Callaghan, NSW, Australia
37 PRC for Health Behaviour, Hunter Medical Research Institute, New Lambton Heights, NSW, Australia
38 Hunter New England Mental Health Service, Newcastle, NSW, Australia
39 Melbourne Neuropsychiatry Centre, Department of Psychiatry, University of Melbourne, Carlton South, VIC, Australia
40 Department of Neuroscience and Physiology, Upstate Medical University, Syracuse, NY, USA
41 Early Psychosis Department, Department of Psychiatry, Amsterdam UMC (location AMC), Amsterdam, The Netherlands
42 Arkin Institute for Mental Health, Amsterdam, The Netherlands
43 Department of Psychiatry and Psychotherapy, Philipps-Universität Marburg, Marburg, Germany
44 Center for Mind, Brain and Behavior (CMBB), Marburg, Germany
45 Core-Facility Brainimaging, Faculty of Medicine, Philipps-Universität Marburg, Marburg, Germany
46 Section for Experimental Psychopathology and Neuroimaging, Department of General Psychiatry, Heidelberg University, Heidelberg, Germany
47 Department of Psychiatry, Perelman School of Medicine, University of Pennsylvania, Philadelphia, PA, USA
48 Lifespan Brain Institute, University of Pennsylvania & Children's Hospital of Philadelphia, Philadelphia, PA, USA
49 Center for Biomedical Image Computing and Analytics, Perelman School of Medicine, University of Pennsylvania, Philadelphia, PA, USA
50 Department of Psychiatry and Neuroscience, University of New Mexico, Albuquerque, NM, USA
51 Department of Psychiatry and Behavioral Sciences and Weill Institute for Neurosciences, University of California, San Francisco, CA, USA
52 Mental Health Service, Veterans Affairs San Francisco Healthcare System, San Francisco, CA, USA
53 Department of Psychiatry and Human Behavior, University of California Irvine, Irvine, CA, USA
54 Psychology Department and Neuroscience Institute, Georgia State University, Atlanta, GA, USA
55 Tri-Institutional Center for Translational Research in Neuroimaging and Data Science (TReNDS), Georgia State University, Georgia Institute of Technology and Emory University, Atlanta, GA, USA
56 San Francisco VA Medical Center, University of California, San Francisco, CA, USA
57 Long Beach VA Health Care System, Long Beach, CA, USA
58 Beijing Huilongguan Hospital, Peking University Huilongguan Clinical Medical School, Beijing, P.R. China
59 Chongqing University Three Gorges Hospital, Chongqing, P.R. China

60 Division of Psychological and Social Medicine and Developmental Neurosciences, Translational Developmental Neuroscience Section, Technische Universität Dresden, University Hospital C.G. Carus, Dresden, Germany
61 Department of Child and Adolescent Psychiatry, Eating Disorder Treatment and Research Center, Technische Universität Dresden, Faculty of Medicine, University Hospital C. G. Carus, Dresden, Germany
62 FIDMAG Germanes Hospitalàries Research Foundation, Barcelona, Spain
63 Mental Health Research Networking Center (CIBERSAM), Madrid, Spain
64 Benito Menni Complex Assistencial en Salut Mental, Barcelona, Spain
65 Laboratory of Neuropsychiatry, IRCCS Santa Lucia Foundation, Rome, Italy
66 Menninger Department of Psychiatry and Behavioral Sciences, Baylor College of Medicine, Houston, TX, USA
67 Department of Psychiatry and Neuropsychology, School for Mental Health and Neuroscience, Maastricht University Medical Centre, Maastricht University, Maastricht, The Netherlands
68 Campbell Family Mental Health Institute, Centre for Addiction and Mental Health, Toronto, Canada
69 Department of Psychiatry, University of Toronto, Toronto, Canada
70 West Region, Institute of Mental Health, Singapore, Singapore
71 Yong Loo Lin School of Medicine, National University of Singapore, Singapore, Singapore
72 Department of Psychosis Studies, Institute of Psychiatry, Psychology and Neuroscience, King's College London, London, United Kingdom
73 Department of Psychological Medicine, Institute of Psychiatry, Psychology and Neuroscience, King's College London, London, United Kingdom
74 Department of Psychiatry, Jeonbuk National University Medical School, Jeonju, Republic of Korea
75 Research Institute of Clinical Medicine, Jeonbuk National University-Biomedical Research Institute, Jeonbuk National University Hospital, Jeonju, Republic of Korea
76 Department of Psychiatry, University Psychiatric Clinics (UPK), University of Basel, Basel, Switzerland
77 Department of Psychiatry and Psychotherapy, University of Lübeck, Lübeck, Germany
78 Division of Psychiatry, Centre for Clinical Brain Sciences, University of Edinburgh, Edinburgh, United Kingdom
79 Department of Psychiatry, Faculty of Medicine and Health Sciences, Stellenbosch University, Stellenbosch, South Africa
80 Stellenbosch University Genomics of Brain Disorders Research Unit, South African Medical Research Council, Cape Town, South Africa
81 Department of Psychiatry and Mental Health, Faculty of Health Sciences, University of Cape Town, Cape Town, South Africa
82 Neuroscience Institute, University of Cape Town, Cape Town, South Africa
83 Institute for Translational Psychiatry, Westfälische Wilhelms-Universität Münster, Münster, Germany
84 The Mind Research Network, Albuquerque, NM, USA
85 Department of Education, Psychology, Communication, University of Bari Aldo Moro, Bari, Italy
86 Department of Basic Medical Science, Neuroscience and Sense Organs, University of Bari Aldo Moro, Bari, Italy
87 Psychiatry Unit, Bari University Hospital, Bari, Italy
88 Department of Child and Adolescent Psychiatry, Institute of Psychiatry and Mental Health, Hospital General Universitario Gregorio Marañón, Madrid, Spain
89 Ciber del Área de Salud Mental (CIBERSAM), Instituto de Salud Carlos III, Madrid, Spain
90 Instituto de Investigación Sanitaria Gregorio Marañón (IiSGM), Madrid, Spain
91 School of Medicine, Universidad Complutense, Madrid, Spain
92 Laboratory of Neuroimaging and Multimodal Analysis, Mental Health Research Center, Moscow, Russian Federation
93 Department of Medical Sciences, Psychiatry, Uppsala University, Uppsala, Sweden
94 Department of Physiology and Pharmacology, Karolinska Institutet, Stockholm, Sweden
95 Department of Psychiatry, Psychotherapy and Psychosomatics, Psychiatric University Hospital Zurich (PUK), Zurich, Switzerland
96 Montreal Neurological Institute, McGill University, Montreal, Canada
97 Department of Psychiatry, Division of Adult Psychiatry, Geneva University Hospitals, Geneva, Switzerland
98 National Institute of Mental Health, Klecany, Czech Republic
99 Department of Psychiatry, Dalhousie University, Halifax, Canada
100 MR Unit, Department of Diagnostic and Interventional Radiology, Institute for Clinical and Experimental Medicine, Prague, Czech Republic
101 Department of Neuropsychiatry, Seoul National University Hospital, Seoul, Republic of Korea
102 Department of Psychiatry, Seoul National University College of Medicine, Seoul, Republic of Korea
103 Department of Brain and Cognitive Sciences, Seoul National University College of Natural Sciences, Seoul, Republic of Korea
104 Department of Psychiatry, University of Oxford, Oxford, United Kingdom
105 Department of Psychiatry, Psychosomatic Medicine and Psychotherapy, University Hospital Frankfurt, Frankfurt am Main, Germany
106 Department of Child and Adolescent Psychiatry, Technische Universität Dresden, Dresden, Germany
107 SA MRC Unit on Risk & Resilience in Mental Disorders, University of Cape Town, Cape Town, South Africa
108 Research Group in Psychiatry (GIPSI), Department of Psychiatry, Faculty of Medicine, Universidad de Antioquia, Medellín, Colombia
109 Experimental Psychopathology and Psychotherapy, Department of Psychology, University of Zurich, Switzerland
110 Center for Psychiatric Neuroscience, Feinstein Institute for Medical Research, Manhasset, NY, USA
111 Division of Psychiatry Research, Zucker Hillside Hospital, Northwell Health, New York, NY, USA
112 Department of Psychiatry, Zucker School of Medicine at Northwell/Hofstra, Hempstead, NY, USA

113 Donders Institute for Brain, Cognition and Behaviour, Radboud University, Nijmegen, The Netherlands
114 Department of Human Genetics, Radboud University Medical Center, Nijmegen, The Netherlands
115 Department of Psychiatry, Radboud University Medical Center, Nijmegen, The Netherlands
116 Department of Psychiatry, Boston Children's Hospital and Harvard Medical School, Boston, MA, USA
117 Olin Neuropsychiatry Research Center, Institute of Living, Hartford, CT, USA
118 Department of Radiology, Perelman School of Medicine, Philadelphia, PA, USA
119 Department of Neurology, Perelman School of Medicine, Philadelphia, PA, USA
120 Imaging Genetics Center, Mark & Mary Stevens Neuroimaging & Informatics Institute, Keck School of Medicine, University of Southern California, Los Angeles, CA, USA
121 School of Psychology, University of Auckland, Auckland, New Zealand
122 Department of Women's and Children's Health, Uppsala University, Uppsala, Sweden
123 Laboratory of Neuro Imaging, School of Medicine, University of Southern California, Los Angeles, USA
124 Psychiatric Genetics, QIMR Berghofer Medical Research Institute, Brisbane, QLD, Australia
125 Clinical Translational Neuroscience Laboratory, Department of Psychiatry and Human Behavior, University of California Irvine, Irvine, CA, USA
126 Center for the Neurobiology of Learning and Memory, University of California Irvine, Irvine, CA, USA

* **Corresponding author:** Clyde Francks, D.Phil., Wundtlaan 1, 6525 XD Nijmegen, The Netherlands; e-mail: Clyde.Francks@mpi.nl; telephone: +31 (0)24-3521929

Abstract

Left-right asymmetry is an important organizing feature of the healthy brain that may be altered in schizophrenia, but most studies have used relatively small samples and heterogeneous approaches, resulting in equivocal findings. We carried out the largest case-control study of structural brain asymmetries in schizophrenia, using MRI data from 5,080 affected individuals and 6,015 controls across 46 datasets in the ENIGMA consortium, using a single image analysis protocol. Asymmetry indexes were calculated for global and regional cortical thickness, surface area, and subcortical volume measures. Differences of asymmetry were calculated between affected individuals and controls per dataset, and effect sizes were meta-analyzed across datasets. Small average case-control differences were observed for thickness asymmetries of the rostral anterior cingulate and the middle temporal gyrus, both driven by thinner left-hemispheric cortices in schizophrenia. Analyses of these asymmetries with respect to the use of antipsychotic medication and other clinical variables did not show any significant associations. Assessment of age- and sex-specific effects revealed a stronger average leftward asymmetry of pallidum volume between older cases and controls. Case-control differences in a multivariate context were assessed in a subset of the data (N = 2,029), which revealed that 7% of the variance across all structural asymmetries was explained by case-control status. Subtle case-control differences of brain macro-structural asymmetry may reflect differences at the molecular, cytoarchitectonic or circuit levels that have functional relevance for the disorder. Reduced left middle temporal cortical thickness is consistent with altered left-hemisphere language network organization in schizophrenia.

Introduction

Schizophrenia is a serious mental illness characterized by various combinations of symptoms that may include delusions, hallucinations, disorganized speech, affective flattening, avolition, and executive function deficits (1). Left-right asymmetry is an important feature of human brain organization for diverse cognitive functions – for example, roughly 90% of people present with a left-hemisphere dominance for language and right-handedness (2-5). A possible role of altered structural and functional brain asymmetry in schizophrenia has been studied for several decades (6-10). Theoretical work has especially focused on disrupted laterality for language in relation to disorganized speech perception and production – the former may sometimes result in auditory verbal hallucinations which are a relatively prevalent symptom (11-14). Individuals with schizophrenia have been reported to show decreased left-lateralized language dominance (15, 16), as well as an absence or even reversal of structural asymmetries of language-related regions around the Sylvian fissure (which divides the temporal lobe from the frontal and parietal lobes) (13, 17-19). Language disturbances such as idiosyncratic semantic associations or reduced grammatical complexity are also commonly reported (20). Furthermore, the rate of non-right-handedness in schizophrenia is elevated compared to the general population (13, 21-25). Interestingly, some genomic loci that influence aspects of structural brain asymmetry or hand preference overlap with those associated with schizophrenia (26-29). Thus, there might be an etiological link between altered brain asymmetry and schizophrenia.

However, alterations in structural asymmetry of the cerebral cortex in schizophrenia have so far only been reported in studies with relatively small samples (13, 17-19, 30-36); to our knowledge, the largest case-control sample consisted of 167 affected individuals and 159 controls (33). Many of the existing findings are inconsistent and/or remain unreplicated, which is possibly due to low statistical power which limits the sensitivity to detect true effects, and also increases the risk of overestimating effect sizes (37-39). The reproducibility of findings may be further affected by the heterogeneity of clinical and demographic characteristics across studies. Moreover, varying approaches to process and analyze magnetic resonance imaging (MRI) data limit the possibility to reproduce results and/or to perform meta-analyses. For example, in studies targeting specific regions of interest, regions have been inconsistently defined, while studies that involved cortex-wide mapping used different image analysis protocols. Studies of subcortical volumetric asymmetries in schizophrenia have generally suffered from similar issues (40-42), with the notable exception of a study in 884 affected individuals and 1,680 controls that used a single image analysis pipeline (43). This study found an increased leftward asymmetry of the pallidum in schizophrenia (driven by a larger pallidum volume in the left hemisphere) compared to controls, which was also detectable in adolescents with subclinical psychotic experiences (43, 44).

The Enhancing Neuro Imaging Genetics through Meta-Analysis (ENIGMA, http://enigma.ini.usc.edu) consortium aims to perform large-scale analyses by combining imaging data from research groups across the world, processed with standardized protocols (45, 46). Previously, this consortium reported large-scale cortical thinning, smaller surface area, and altered subcortical volume in individuals with schizophrenia compared to controls (47, 48). However, asymmetry was not measured in these previous ENIGMA studies, and no tests were performed to assess whether case-control effects were different in the two hemispheres. The ENIGMA consortium has investigated structural brain asymmetries in other disorders (49): major depressive disorder (MDD) (50), autism spectrum disorder (ASD) (51), obsessive compulsive disorder (OCD) (52), and attention deficit/hyperactivity disorder (ADHD) (53). Case-control group-level effects were small for all of these disorders, with ASD showing the most widespread asymmetry differences – mostly involving regional cortical thickness measures – with a maximum Cohen's *d* of 0.13 (51). Similar effect sizes may be anticipated for schizophrenia. Therefore, a large sample size is likely required to detect and accurately measure any effects. Although small group-average differences of brain macro-anatomy are unlikely to have clinical uses by themselves, they may help to identify brain regions and networks that have clinically relevant disruptions at other neurobiological levels – for example molecular or cytoarchitectonic – which can be investigated in future studies. Of note, the ENIGMA consortium has recently reported on asymmetry alterations with respect to subcortical *shape* (2,833 individuals with schizophrenia versus 3,929 controls), based on an automated approach quantifying local concave versus convex surface curvature (54), but that study did not address subcortical *volume* asymmetries, and omitted the cerebral cortex.

For the current study, we were able to measure both cortical and subcortical structural asymmetries in schizophrenia using by far the largest sample to date: 5,080 affected individuals and 6,015 controls, from 46 separate datasets. The datasets were collected originally as distinct studies over approximately 25 years, using different recruitment schemes, MRI scanning equipment and parameters. Importantly, for the current study, all primary MRI data were processed through a single pipeline for cortical atlas-based segmentation/subcortical parcellation and quality control.

Given previous theoretical and empirical work linking schizophrenia to reduced language laterality and function (see above), we had a particular interest in whether typical structural asymmetries of the core cerebral cortical language network might be reduced in schizophrenia – this includes asymmetries of lateral temporal cortex and inferior frontal cortex (55). However, linguistic tasks can also recruit various other brain regions (56), while disrupted cognition in schizophrenia affects multiple domains beyond language (1). Our primary aim was therefore to map potentially altered structural asymmetry in schizophrenia across all cortical and subcortical regions, for a thorough and unconstrained mapping of brain asymmetry in schizophrenia, supported by our unprecedented sample size. We achieved this through separate region-by-region testing of case-control group average differences in asymmetry

(followed by false discovery rate correction), where the testing was two-tailed, i.e. we allowed for either reductions, increases or even reversals of asymmetry in affected individuals compared to controls. Due to restrictions on sharing individual-level data for many of the primary datasets, case-control differences were first tested for each regional asymmetry index (AI) separately within each dataset, and effects were then combined across datasets using meta-analysis methodology.

We also performed various secondary/exploratory analyses of the data. We explored possible associations of structural brain asymmetries with medication use and other disorder-specific measures: age at onset, duration of illness, as well as total, positive, and negative symptom scores. In addition, we tested age- and sex-specific asymmetry differences. Finally, for 14 datasets for which individual-level data were available, we tested for a multivariate association of case-control status simultaneously with regional AIs across the brain.

Together, these analyses aimed to provide novel insights into the extent and mapping of structural brain asymmetry alterations in schizophrenia, and how they relate to key clinical variables.

Methods and materials

Datasets

Structural MRI data were derived from 46 separate datasets (45 case-control and one case-only) via researcher participation in the ENIGMA schizophrenia working group, totaling 11,095 individuals. Of these, 5,080 were affected with schizophrenia and 6,015 were unaffected controls (Table 1, Table S1A). The datasets came from various countries around the world and were collected over the last roughly 25 years (Fig. 1). For each of the datasets, all relevant local ethical regulations were complied with, and appropriate informed consent was obtained for all individuals. The present study was carried out under approval from the Ethics Committee Faculty of Social Sciences of Radboud University Nijmegen. Sample size-weighted mean age across datasets was 33.3 (range 16.2-44.0) years for individuals with schizophrenia and 33.0 (11.8-43.6) years for controls. Affected individuals and controls were 67% and 52% male, respectively. Diagnostic interviews were conducted by registered clinical research staff using different diagnostic criteria (either the Diagnostic and Statistical Manual of Mental Disorders [DSM]-III, DSM-IV, DSM-5 or International Classification of Diseases [ICD]-10), and hand preference was obtained through assessment scales (mainly the Edinburgh Handedness Inventory and Annett Handedness Scale) or self-report (Table S2). No controls had present or past indications of schizophrenia.

Image acquisition, processing and quality control

T1-weighted structural brain MRI scans were acquired at each study site. Dataset-specific scanner information, field strengths (1 T, 1.5 T, and 3 T), and image acquisition parameters are provided in Table S2. For data from all sites, image processing and segmentation were performed using FreeSurfer (see Table S2 for software versions) (57). For each individual, using the 'recon-all' pipeline, cerebral cortical thickness and surface area measures were derived for 34 bilaterally paired Desikan-Killiany (DK) atlas regions, as well as whole hemisphere-level average cortical thickness and surface area measures (58). Volumes for 8 bilaterally paired regions from a neuroanatomical atlas of brain subcortical structures (59) were derived using the 'aseg' segmentation command in FreeSurfer. A standardized ENIGMA quality control procedure was applied at each participating site (described in full here: http://enigma.ini.usc.edu/protocols/imaging-protocols/). Briefly, this included outlier detection in the derived cortical and subcortical measures and visual inspection of segmentations projected onto the T1-weighted image of each individual. For cortical measures, predefined guidelines for visual inspection were followed. Measurements from regions with poor segmentation were excluded, as well as individuals whose data failed overall quality checks. Data sharing limitations did not allow the central analysis group to have access to individual-level data for the majority of participating study sites. For further processing and analyses of the data, a script running in R software (R Foundation for Statistical Computing, Vienna, Austria, www.R-project.org) (60) was prepared and distributed among participating sites, to ensure coordinated collection of descriptive and summary statistics for subsequent meta-analysis by the central analysis team.

Asymmetry index calculation

For each bilaterally paired brain regional measure, we used the left (L) and right (R) hemispheric measurements to calculate $AI = \frac{L-R}{(L+R)/2}$, where the denominator corrects for automatic scaling of the index with the magnitude of the bilateral measure. This formula for AI calculation has been widely used (2, 52, 61-63). A negative value of the AI reflects a larger right hemispheric measurement ($R > L$), and a positive value a larger left hemispheric measurement ($L > R$). Distributions of AIs were plotted using histograms to allow for visual inspection. Left or right measurements equal to 0 were set to missing, as these most likely reflected data entry errors. Furthermore, when a left or right measurement was missing, the corresponding measurement in the opposite hemisphere was also set to missing. The standardized pipeline from raw image data through FreeSurfer does not introduce left-right flipping errors, but to ensure that such errors were not introduced during processing of raw imaging data by non-standard processes (e.g. during the conversion of DICOM to NIFTI files with bespoke scripts), we compared mean regional asymmetries for all datasets against grand sample-size adjusted means. If we noticed a large proportion of reversed average asymmetries for a dataset, we contacted the relevant site to re-check and correct their process (Table S3).

Asymmetry differences between individuals with schizophrenia and unaffected controls

Group differences were examined separately for each brain regional AI and each case-control dataset, using univariate linear regression implemented in R. Our primary analysis model included diagnosis (case-control status) as the main binary predictor, and sex and age as covariates (model 1 in Supporting Information 1). For ten datasets where more than one scanner had been used (Table S2), we added *n*-1 binary dummy covariates (where *n* is the number of scanners in a given dataset), to statistically control for scanner effects. Sex was not included as a covariate for the RSCZ dataset, as this dataset included only males. Collinearity between predictor variables was assessed using the R-package *usdm* (v1-1.18) (64), and high collinearity (variance inflation factor > 5) was not found for any dataset. Linear regression analysis for any structural AI was not performed if the total sample size of a given dataset was lower than ten plus the number of scanner covariates, or if one of the diagnostic groups had a sample size lower than five. For each brain regional AI and each case-control dataset, we extracted the *t*-statistic for the 'diagnosis' term to calculate its corresponding Cohen's *d* effect size, standard error and 95% confidence interval, using $d = \frac{t(n_1+n_2)}{\sqrt{n_1 n_2}\sqrt{df}}$, $se_d = \sqrt{\left(\frac{n_1+n_2-1}{n_1+n_2-3}\right)\left[\left(\frac{4}{n_1+n_2}\right)\left(1+\frac{d^2}{8}\right)\right]}$, and 95% $CI = [d - 1.96 * se_d, d + 1.96 * se_d]$ (65). In these equations, *d* is the Cohen's *d* effect size, *t* is the *t*-statistic, *se* is the standard error, n_1 is the number of unaffected controls, n_2 is the number of individuals with schizophrenia, and *df* the degrees of freedom in the linear model.

Random-effects meta-analysis

For each brain regional AI (Fig. S1-S3), effect sizes for 'diagnosis' from each case-control dataset were meta-analyzed in a random-effects model fitted with a restricted maximum likelihood (REML) estimator, using the function 'rma' in the R package *metafor* (v3.0-2) (66). Meta-analyzed effect sizes were projected on 3D meshes of inflated cortical or subcortical models from Brainder (www.brainder.org/research/brain-for-blender/), using Matlab R2020a (version 9.8.0.1323502; MathWorks, Natick, MA, USA). We calculated false discovery rate (FDR) corrected p-values using the Benjamini-Hochberg method to account for multiple tests (67) (i.e., separately for testing 35 cortical thickness AIs, 35 cortical surface area AIs, and eight subcortical volume AIs). Effects with $p_{FDR} < 0.05$ were considered statistically significant. For AIs that showed significant group differences between cases and controls, the group differences for the corresponding left and right measurements separately were also assessed *post hoc* (again using linear modelling with diagnosis, age and sex as predictors), to help describe the asymmetry differences.

Sensitivity analyses

For any AI that showed a significant case-control group difference in the primary meta-analysis, we carried out three types of sensitivity analyses:

First, we identified datasets within which the 95% CI of the diagnosis effect did not overlap with the 95% CI of the meta-analyzed effect – using the 'find.outliers' function in the R package *dmetar* (v0.0.9) (68) – and then repeated the meta-analysis after excluding such outlier datasets.

Second, to assess whether between-dataset heterogeneity in effect sizes could be partly explained by known aspects of technical, diagnostic or geographic variability between datasets, we applied meta-regression and the Cochran's Q test. As possible moderators we tested scanner strength, scanner manufacturer, use of a single scanner versus multiple scanners, image slice orientation, FreeSurfer version, diagnostic tool, and geographic origin of datasets (ethnicity was not recorded). See Table S2 for more information on these possible moderators.

Third, we applied models that included the same covariates as the primary analysis, but additionally included either handedness (right-handed vs. non-right-handed), intracranial volume (ICV), both handedness and ICV, or age^2 (models 2-5 in Supporting Information 1).

Medication group differences

For AIs that showed significant case-control group differences in the primary analysis, we explored associations with antipsychotic medication use at the time of scanning, through between-group comparisons of AIs of unmedicated individuals with schizophrenia, affected individuals taking only first-generation (typical) antipsychotics, affected individuals taking only second-generation (atypical) antipsychotics, and those taking both first- and second-generation antipsychotics. Sex and age were included as covariates (model 6 in Supporting Information 1) and derived Cohen's *d* effect sizes were again meta-analyzed across datasets in a random-effects model. Applying a minimum group size threshold of 5 within any given dataset, sufficient data on the presence/absence of antipsychotic medication use for at least one comparison were available for 31 of the datasets (Table S1B), and the sample sizes for each between-group comparison are in Table S9. We calculated FDR corrected p-values to correct for all of the multiple subgroup comparisons and structural asymmetries tested.

Correlations of asymmetries with clinical variables

For AIs that showed significant case-control group differences in the primary analysis, we assessed relationships between these AIs and clinical variables within affected individuals only: age at onset, duration of illness, chlorpromazine equivalent medication dose (at the time of scanning), as well as positive, negative, and total symptom severity scores from the Positive and Negative Symptom Scale (PANSS) (69), or the Scale for the Assessment of Positive Symptoms (SAPS) (70) and Scale for the Assessment of Negative Symptoms (SANS) (71) (separately depending on data availability, see Table S1A). Partial correlations between brain AIs and these quantitative measures were estimated using the 'pcor.test' function in the R package *ppcor* (v1.1) (72). Age and sex were included as covariates (model 7 in Supporting Information 1). The same minimum sample size requirement for dataset inclusion was

applied as in the linear regression analyses (above). Correlation coefficients were meta-analyzed across datasets in a mixed-effects model including dataset as a random effect. We calculated FDR corrected p-values to control for all of the clinical variables and structural asymmetries tested. Sample sizes for each model are shown in Table S10.

Secondary analysis of age- or sex-specific effects

For all AIs in all case-control datasets we applied models which were the same as the primary analysis but additionally included either diagnosis-by-age or diagnosis-by-sex interaction terms. We then carried out meta-analyses of the interaction effect estimates across datasets to assess possible AI differences between affected individuals and controls that were relatively specific to either males or females, or differed with age (models 8-9 in Supporting Information 1). In the same way as our primary analysis, we calculated FDR corrected p-values to account for multiple regional asymmetries tested.

Multivariate analysis of case-control asymmetry differences

To examine case-control group differences across all brain regional AIs simultaneously in one model, we conducted a multivariate analysis based on 14 datasets for which individual-level data were available to the central analysis team. For this analysis, we only retained individuals with complete data for all bilateral measures of cortical and subcortical structures, which were 935 individuals affected with schizophrenia and 1,095 unaffected controls (Table S1C). We separately adjusted the left and right measurements using ComBat harmonization (an empirical Bayesian method) to remove dataset effects (73), where each dataset (and each scanner within multi-scanner datasets) was treated as a distinct 'batch'. Diagnosis, age and sex were used as covariates when finding the data harmonization parameters in ComBat. After ComBat adjustment, one additional control individual was removed due to being assigned a negative corrected right hemisphere lateral ventricle volume (Fig. S4). AIs for cortical and subcortical measures were then calculated using the same formula as above, and collinearity between AIs was assessed by calculating a correlation matrix. AIs did not show higher pairwise correlations than 0.5 (Fig. S5-S6) A multivariate analysis of covariance (MANCOVA) using the 'manova' function in R was applied, testing all 76 regional structural brain AIs simultaneously against case-control status, with age and sex as covariates. We ran one million label-swapping permutations of case-control labels and calculated a permutation *p*-value by assessing the number of times the *F*-statistic of an analysis with permuted data was equal to or larger than the *F*-statistic of the analysis with real data, divided by the total number of permutations. When permuting case-control labels, we conserved case-control numbers within each dataset (and within scanner for multi-scanner datasets). To help interpret the MANCOVA results, we also derived univariate case-control association statistics for each separate structural AI from the multivariate association analysis output, using ANCOVA ('summary.aov' function in R).

Results

Asymmetry differences between individuals with schizophrenia and unaffected controls

In our primary analysis (model 1), total hemispheric average cortical thickness asymmetry (d = -0.053, z = -1.92, p = 0.055) and surface area asymmetry (d = 0.027, z = 1.23, p = 0.22) did not significantly differ between affected individuals and controls. At a regional level (Fig. 2, Table S4, Fig. S1-S3), there was a small but significant case-control difference in cortical thickness asymmetry of the rostral anterior cingulate cortex (d = -0.083, z = -3.21, $p = 1.3 \times 10^{-3}$, p_{FDR} = 0.047, reversal from leftward average asymmetry in controls to rightward average asymmetry in cases), and also in cortical thickness asymmetry of the middle temporal gyrus (d = -0.074, z = -2.99, $p = 2.8 \times 10^{-3}$, p_{FDR} = 0.048, increased average rightward asymmetry in cases) (Fig. 3, Fig. S7-S8, Table S5). *Post hoc* analysis of unilateral effects showed that both of these regional asymmetry differences were driven primarily by thinner left than right cortex in individuals with schizophrenia compared to controls (Table 2, Table S6). The middle temporal cortex is a core language network region (56), and left-hemisphere thinning is compatible with disrupted leftward laterality of brain organization for language in schizophrenia (10, 11). Nominally significant regional case-control associations (i.e. which did not survive multiple testing correction), were found for the AIs of inferior parietal cortex thickness, cuneus surface area, parahippocampal gyrus surface area, and nucleus accumbens volume (Fig. 3, Table S5).

Sensitivity analyses

For rostral anterior cingulate thickness asymmetry, there were three datasets in the primary meta-analysis which had outlier case-control effect sizes when compared to the meta-analyzed effect (see Methods). After excluding these datasets and repeating the meta-analysis for this AI, the case-control difference remained, with the same directionality (d = -0.073, z = -3.51, $p = 4.5 \times 10^{-4}$) (Table S7). For middle temporal gyrus thickness asymmetry, the exclusion of two outlier datasets also yielded a similar result compared to the primary analysis (d = -0.079, z = -3.44, $p = 5.9 \times 10^{-4}$), again with the same directionality (Table S7).

Meta-regression analysis did not identify any significant moderators (no Cochran's Q omnibus test p-values < 0.05) (Fig. S9-S22), i.e. Cohen's d effect sizes reflecting asymmetry differences between individuals with schizophrenia and unaffected controls were not significantly influenced by scanner strength, scanner manufacturer, use of a single scanner versus multiple scanners, image slice orientation, FreeSurfer version, diagnostic tool, or the geographic origin of datasets.

In models that included either handedness, ICV, both handedness and ICV, or age^2 as additional covariates (models 2-5), the case-control differences for both of these regional AIs remained nominally significant, with similar directions and magnitudes of effect compared to the case-control differences

found in the primary analysis (Table S8), despite differences in sample sizes resulting from limited availability of some of these variables.

Medication group differences

Rostral anterior cingulate thickness asymmetry did not differ between affected individuals across medication groups (model 6) (Table S9). For the middle temporal gyrus, there was a nominally significant increase in average rightward asymmetry in affected individuals taking first generation versus second generation antipsychotics at the time of scanning (d = -0.21, z = -2.56, p = 0.011, p_{FDR} = 0.13), i.e., this was not significant after multiple testing correction (Table S9).

Correlations of asymmetries with clinical variables

We found nominally significant correlations between rostral anterior cingulate thickness asymmetry and negative symptom severity measured with SANS (r = 0.049, z = 2.08, p = 0.038, p_{FDR} = 0.32, decreased rightward asymmetry with higher negative symptom rate) (Table S10A) and between middle temporal gyrus thickness asymmetry and duration of illness (r = -0.048, z = -1.97, p = 0.049, p_{FDR} = 0.32, increased rightward asymmetry with longer duration of illness) (Table S10B), but these correlations did not remain significant when correcting for multiple testing. No correlations with chlorpromazine-equivalent medication dose, age at onset, PANSS scores (total or positive and negative subscales), or SAPS or SANS scores, were found for either the rostral anterior cingulate thickness asymmetry or middle temporal gyrus thickness asymmetry (Table S10).

Age- and sex-specific effects

In secondary analyses across all AIs using models with interaction terms, we found a significant diagnosis-by-age interaction (model 8) for pallidum volume asymmetry (d = 0.081, z = 3.26, p = 1.1 x 10^{-3}, p_{FDR} = 9.0 x 10^{-3}, stronger leftward asymmetry with higher age in cases) (Table S11-S12A, Fig. S23). This association was driven by a significantly decreased average leftward asymmetry with increasing age in controls (r = -0.077, p = 1.1 x 10^{-3}) that was not present in affected individuals (Table S12B; Fig. S24). In terms of the corresponding unilateral effects, left and right pallidum volume decreased with increasing age in individuals with schizophrenia (L: r = -0.17, p = 4.7 x 10^{-9}; R: r = -0.20, p = 4.7 x 10^{-21}) and unaffected controls (L: r = -0.27, p = 2.1 x 10^{-22}; R: r = -0.24, p = 6.2 x 10^{-17}), but the two groups differed with respect to the side showing the stronger effect (Table S12B). No significant sex-by-diagnosis interactions were found (model 9) (Table S13).

Multivariate analysis of case-control asymmetry differences

Considering all 76 regional structural brain AIs simultaneously in a multivariate model, applied to the 14 datasets for which individual-level data were available to the central analysis team (935 affected

individuals and 1,094 controls), there was a significant multivariate structural brain asymmetry difference between cases and controls that accounted for roughly 7% of the variance considered across all 76 AIs (Wilks' $\Lambda = 0.932$, approximate $F(76, 1950) = 1.87$, $p = 1.25 \times 10^{-5}$). Only three of the *F*-statistics resulting from one million label-swapping permutations (see Methods) were larger than the *F*-statistic from the true analysis, resulting in a permutation $p = 3.0 \times 10^{-6}$. We also derived univariate (ANCOVA) association statistics from the multivariate model to understand which AIs contributed most to the significant multivariate association. The structural AIs that showed nominally significant, univariate case-control differences in the 14 datasets available for this analysis were those for pallidum volume, nucleus accumbens volume, and eight regional surface area or thickness measures distributed widely over the cerebral cortex (Table 3). These did not include the two cortical regional AIs that showed significant case-control differences in the meta-analysis over all 45 case-control datasets, but did include AIs of other language-related regions of the temporal lobe: superior temporal sulcus surface area asymmetry and transverse temporal gyrus thickness asymmetry (Table 3). The large differences in overall sample size and contributing datasets between the multivariate analysis and main meta-analysis are a likely cause of these somewhat different results.

Discussion

In this study, we investigated group differences in structural brain asymmetries between individuals with schizophrenia and unaffected controls, in the largest sample to date. The large sample size offered unprecedented statistical power to identify group differences based on the clinical diagnosis of schizophrenia, and to measure their effect sizes (37-39). Subtle differences of regional asymmetry were found for rostral anterior cingulate thickness, middle temporal gyrus thickness, and pallidum volume (the latter in older individuals). The Cohen's *d* effect sizes were less than 0.1; i.e., very small (74). In light of previous large-scale analyses of bilateral cortical and subcortical alterations in schizophrenia (47, 48), our results suggest that morphometric alterations in this disorder are largely the same for the left and right hemispheres, involving only subtle asymmetrical effects at the group average level. This suggests that effect sizes of brain asymmetry differences in schizophrenia reported in earlier, much smaller studies (see Introduction), are likely to have been overestimated. Nonetheless, in a multivariate context, 7% of the total variance across all regional asymmetries was explained by case-control status, indicating a diffuse and subtle alteration of brain asymmetry in schizophrenia.

Subtle group differences of asymmetry in terms of macro-anatomic features, such as those studied here, may reflect effects at other neurobiological levels that have functional relevance for disorder symptoms – for example molecular, cytoarchitectonic and/or circuit levels (75-77). For example, cortical thickness measures can correlate with the degree of myelination (78), such that quantitative neuroimaging

methods that are more sensitive to microstructural tissue content may reveal alterations in the regions implicated by this study. Neurite orientation dispersion and density imaging can be used to study cortical microstructural asymmetries (77), or the ratio of T1w and T2w images in grey matter can indicate cortical myelin content (79). We suggest that future studies using such techniques can be focused on the regions identified in this study. In addition, post mortem studies of hemispheric differences in gene expression in schizophrenia are motivated.

The middle temporal gyrus is prominently involved in the brain's language network (56), so that our finding of lower left-sided cortical thickness in schizophrenia in this region is broadly consistent with a prominent theory in the literature: that left-hemisphere language dominance may be reduced in this disorder (10, 11). Cortical thinning of the left-hemispheric middle temporal gyrus has been associated with auditory verbal hallucinations in schizophrenia (80), and is reported in individuals with first-episode schizophrenia and high familial risk for the disorder (81, 82). In terms of grey matter volume, an opposite pattern (reduced right, increased left) has been reported for the middle temporal gyrus in putatively at-risk children compared to typically developing children (83). However, volume measures confound cortical thickness and surface area, and since these two aspects of cortical anatomy are known to vary substantially independently (28, 84, 85), it is unclear how these earlier volume-based findings may relate to the present findings based on cortical thickness asymmetry. Again, earlier findings in smaller samples may have been false positives with over-estimated effect sizes.

The rostral anterior cingulate cortex is an important hub in emotional and cognitive control (86), both of which are often affected in schizophrenia. In this region we observed a thinner left-sided cortex in affected individuals than controls on average, which was more pronounced than on the right side. This may be consistent with a previous study where adolescent/young adult relatives of individuals with schizophrenia showed a longitudinal decline of gray matter volume in the left rostral anterior cingulate cortex compared to controls (87). It is therefore possible that asymmetrical differences in this region emerge before schizophrenia onset, although the previous study included only 23 relatives, so its reported effects remain equivocal, and it used volume rather than thickness measures. In the present study, we saw no evidence for an age*diagnosis interaction effect for this regional thickness asymmetry, which is consistent with a pre-onset alteration that subsequently remains stable through adulthood.

Multivariate analysis in 14 of the datasets, for which individual-level data were available, resulted in a highly significant case-control difference. Various regional asymmetries contributed to this multivariate association, with pallidum volume asymmetry showing the largest individual contribution. Pallidum volume asymmetry was especially associated with schizophrenia in older individuals, as observed in secondary testing of univariate interaction models across all 45 case-control datasets. Larger pallidum volume in schizophrenia compared to controls – with a stronger effect in the left hemisphere – has been

reported before (43, 44, 48, 88), although some datasets in our analysis partly overlapped with three of these studies (43, 44, 48). An age-dependent relationship between familial risk for schizophrenia and larger left pallidum volume has also been described in a small study of young adults (89) – this suggests that alterations of pallidum asymmetry might already be present in a prodromal stage of the disease. However, in the present study, the group difference in pallidum volume was absent in younger individuals and became more apparent in older adults. This also explains why the association was not significant in the primary univariate meta-analysis of all datasets together, i.e. it was driven by a subset of datasets that included older individuals, and that were also available for multivariate analysis (Fig. S24). The pallidum is prominently involved in reward and motivation (90), and impaired reward anticipation and a loss of motivation are well-known negative symptoms of schizophrenia (91). However, how pallidum structural asymmetry may relate to functional disorder-relevant changes remains unknown.

Various brain regional asymmetries have shown significant heritability in a recent genome-wide analysis of general population data (28), including rostral anterior cingulate thickness asymmetry and pallidum volume asymmetry (but not middle temporal gyrus thickness asymmetry). When polygenic risk for schizophrenia was assessed with respect to these heritable asymmetries in a multivariate analysis (29), one of the strongest associations was with rostral anterior cingulate thickness asymmetry. The direction of that effect was consistent with the present study, i.e. a rightward shift of asymmetry with increased polygenic risk for schizophrenia. In contrast, pallidum volume asymmetry showed little relation to schizophrenia polygenic risk (29), suggesting non-heritable contributions to this association. These genetic findings were established with adult general population data (UK Biobank) (29), but together with the current case-control findings, they indicate that altered rostral anterior cingulate thickness asymmetry may be a link between genetic susceptibility and disorder presentation. Left-right asymmetry of the brain originates during development *in utero* (75, 92-97), and specific genomic loci that affect brain asymmetry have recently been identified (28, 98). Some of the implicated genes may be involved in patterning the left-right axis of the embryonic or fetal brain, and genes expressed at different levels on the left and right sides of the embryonic central nervous system were found to be particularly likely to affect schizophrenia susceptibility (92). However, other genes may affect brain asymmetry as it changes throughout the lifespan (2, 99) and therefore may affect susceptibility to asymmetry-associated disorders later in life.

The magnitudes of effects in this study were in line with those reported in recent large-scale studies of brain asymmetry in other psychiatric disorders carried out through the ENIGMA consortium (50-53). In ASD, a similar decreased leftward asymmetry of rostral anterior cingulate thickness was reported (51) – this region is important in cognitive control which can be impaired in both schizophrenia and ASD. For ADHD, a nominally significant increase in rightward asymmetry of middle temporal gyrus

thickness was reported, while in adults specifically, less leftward asymmetry of pallidum volume was found (53). The former finding is consistent in its direction of effect with the present study, while the latter is opposite. For OCD, the pallidum was found to be less left lateralized in cases versus controls in a pediatric dataset and this effect was again opposite to our current findings in older individuals with schizophrenia (52). These cross-disorder comparisons suggest that clinical and etiological similarities and differences between schizophrenia and other psychiatric disorders might be partly reflected in asymmetry alterations involving some of the same brain regions. For further discussion of brain asymmetry alterations across multiple psychiatric traits, see Mundorf et al. (100).

Schizophrenia is a highly heterogeneous disorder covering a range of possible symptoms, which may correspond to differing underlying disease mechanisms. Our primary analysis only considered case-control group average differences based on the overall diagnosis of schizophrenia, and in secondary analyses, we did not find significant correlations of asymmetries with major clinical variables within cases after adjusting for multiple testing - including age at onset, duration of illness, and symptom scores. Furthermore, data for several variables were only available from a limited number of study sites (medication, handedness, clinical variables), reducing the sample size and thus statistical power in these secondary analyses. More detailed clinical data would be useful to gather in future large-scale studies of structural asymmetries. For example, a future study could investigate middle temporal gyrus thickness asymmetry in relation to the presence and severity of auditory verbal hallucinations (note that PANSS question 3 does not distinguish between auditory, visual, olfactory or somatic types of hallucination, so a more targeted clinical assessment would be required).

This was the largest study of structural brain asymmetries in schizophrenia to date, and made use of a single image processing and analysis pipeline to support analysis across multiple datasets. The fact that we used data from a range of imaging equipment, diagnostic tools and regions of the world ensures generalizability of our findings, as they pertain to the diverse manner in which schizophrenia is diagnosed and studied internationally. Therefore, a major strength of our approach is in showing consensus effects across inter-site variations in techniques and samples. Unlike in a highly selected, single site or single equipment study, the broad and generalizable total dataset made it unlikely that any single factor confounded our findings. We used a meta-analytic approach after testing for effects separately within each dataset, where cases and controls were matched for technical and demographic factors within each dataset. This allowed us to assume and control for variations between datasets in our main analysis. In addition, meta-regression analyses indicated that between-dataset variability in technical, diagnostic or geographic aspects had no significant impact on the associations between schizophrenia and regional brain asymmetries identified in this study. It is also worth noting that several findings from the ENIGMA-Schizophrenia working group (not related to asymmetry) have been

replicated by The Cognitive Genetics Collaborative Research Organization (COCORO) in a sample collected in Japan (101), supporting generalization of findings across populations.

We used cross-sectional datasets, limiting the possible interpretation with respect to cause-effect relations, longitudinal changes in asymmetry, or medication effects on asymmetry. Many of the individuals with schizophrenia were likely to be past or current users of medication, although data on medication were only available for a subset of datasets, and were also limited to medication use at the time of scanning. We found no evidence that the asymmetries of rostral anterior cingulate thickness or middle temporal gyrus thickness were different in affected individuals using medication versus those not using medication, which may indicate that the case-control differences of asymmetry that we detected had a developmental origin, rather than reflecting medication use. Indeed, medication effects on cortical thickness may be predominantly bilateral, without necessarily affecting asymmetry. We are not aware of any comparably sized prospective/randomized study in which medication effects could be disentangled from case-control effects.

We found a tentative difference of middle temporal gyrus thickness asymmetry between individuals who were taking first-generation versus second-generation antipsychotics. In principle this finding might reflect a change of asymmetry in response to first generation medication in particular, or else clinical differences of disorder presentation linked to asymmetry which then affect treatment choices. We saw nominally significant evidence that this same regional asymmetry relates to illness duration. However, the medication subgroup analyses were limited by relatively small sample sizes compared to the primary case-control analysis, and this particular association did not survive multiple testing correction. Also, medication status did not include information on previously used antipsychotics. This association therefore remains uncertain until replicated.

We used macro-anatomical brain atlases for both the cortical and subcortical structures, which is the most feasible approach for large-scale analysis across multiple datasets, but limits spatial resolution. With higher resolution mapping, regions that showed negative results in our study may harbor more focal case-control asymmetry differences, which could be revealed for example through vertex-wise cortical mapping (63, 98, 102), or subcortical partitioning into subfields or nuclei.

This study focused on group average differences, but individual-level deviations in affected individuals may be highly heterogeneous and not well captured by group-average approaches (103). Future studies may investigate individual or patient subgroup asymmetry deviations from a normative range or structural pattern, which may deliver clinical utility, for example through contributing to diagnosis or prognosis. This concept has shown promising results in recent studies even in smaller samples (103, 104). The small group-average effects that we identified in the present study are unlikely to have clinical

utility when considered in isolation, although they may contribute to multivariate prediction models in future research, for example when considering brain features across multiple imaging modalities.

In summary, we performed the largest study of asymmetry differences between individuals with schizophrenia and unaffected controls to date. Effect sizes were small, but several regional case-control asymmetry differences in cortical thickness and subcortical volume were suggested, and multivariate analysis indicated that 7% of variation across all regional asymmetries could be explained by the case-control group difference. Our findings therefore support a long-standing theory that the brain's asymmetry can be different in schizophrenia (10, 11), even if earlier studies in smaller samples were likely to have over-estimated the effect sizes in relation to structural asymmetry. Altered asymmetry in schizophrenia may conceivably occur during development through disruption of a genetically regulated program of asymmetrical brain development, and/or through different trajectories of lifespan-related changes in brain asymmetries. The specific regions implicated here provide targets for future research on the molecular and cellular basis of altered lateralized cognitive functions in schizophrenia, which may ultimately help to identify pathophysiological mechanisms.

Acknowledgments

The ENIGMA project is in part supported by the National Institute of Biomedical Imaging and Bioengineering of the National Institutes of Health (NIH) (Grant No. U54EB020403). The content is solely the responsibility of the authors and does not necessarily represent the official views of the NIH. D.S., M.C.P., S.E.F. and C.F. [ENIGMA-Laterality] were funded by the Max Planck Society (Germany). R.A-A. [PAFIP] is funded by a Miguel Servet contract from the Carlos III Health Institute (CP18/00003). J.V-B. [PAFIP] has received unrestricted research funding from Instituto de Investigación sanitaria Valdecilla (IDIVAL): INT/A21/10, INT/A20/04. D.A. [TOP] is funded by the South-Eastern Norway Regional Health Authority (grants 2019107 and 2020086). L.T.W. [TOP] is funded by The Research Council of Norway (223273, 300767), the South-Eastern Norway Regional Health Authority (2019101), and the European Research Council under the European Union's Horizon 2020 research and Innovation program (ERC StG, Grant 802998). O.A.A. [TOP] is funded by the Research Council of Norway (#223273, #275054) and KG Jebsen Stiftelsen, South East Norway Health Authority (2017-112, 2019-108). P.K. [MPRC, Huilong] received support from NIH grants R01MH123163 and R01EB015611. M.J.G. [ASRB, IGP] received funding from National Health and Medical Research Council (NHMRC) Project Grants 630471, 1051672, 1081603. C.P. [ASRB] was supported by a NHMRC Senior Principal Research Fellowship (1105825), and NHMRC L3 Investigator Grant (1196508). V.D.C. [FBIRN, COBRE] was funded by NIH grants R01MH118695 and National Science Foundation (NSF) 2112455. J.M.F. [FBIRN] was funded by a Senior Research Career Scientist Award, Department of Veterans Affairs. P.F-C. [FIDMAG] is funded by Centro de Investigación Biomédica en Red de Salud Mental (CIBERSAM) and by Instituto de Salud Carlos III, co-funded by European Union (European Regional Development Fund (ERDF)/European Social Fund (ESF), 'Investing in your future'): Sara Borrell Research contract (CD19/00149). G.S. [RomeSL] was funded by Italian Ministry of Health RC17-18-19-20-21/A grants. A.N.V. [CAMH] currently receives funding from the National Institute of Mental Health, Canadian Institutes of Health Research, Canada Foundation for Innovation, Centre for Addiction and Mental Health (CAMH) Foundation, and the University of Toronto. K.S. [IMH] received support from research grants from the National Healthcare Group, Singapore (SIG/05004; SIG/05028), and the Singapore Bioimaging Consortium (RP C009/2006). Y-C.C. [JBNU] was supported by a grant of the Korean Mental Health Technology R&D Project, Ministry of Health & Welfare, Republic of Korea (HL19C0015) and a grant of the Korea Health Technology R&D Project through the Korea Health Industry Development Institute (KHIDI), funded by the Ministry of Health & Welfare, Republic of Korea (HI18C2383). U.D. [FOR2107 Münster] was funded by the German Research Foundation (DFG, grant FOR2107 DA1151/5-1 and DA1151/5-2; SFB-TRR58, Projects C09 and Z02) and the Interdisciplinary Center for Clinical Research (IZKF) of the medical faculty of Münster (grant Dan3/012/17). J.M.S. [COBRE] was funded by NIH grant 1P20RR021938-01. A.R.M. [COBRE] received funding from NIH grants P30GM122734 and

R01MH101512. C.M.D-C. [Madrid] has received funding from Instituto de Salud Carlos III, Spanish Ministry of Science and Innovation (PI17/00481, PI20/00721, JR19/00024). S.Ce. [KaSP] received funding from the Swedish Research Council (Grant No. 523-2014-3467). M.Kir. [Zurich] acknowledges funding from the Swiss National Science Foundation (P2SKP3_178175). T.H. [ESO] was supported by funding from the Canadian Institutes of Health Research (142255), Ministry of Health of the Czech Republic (16-32791A, NU20-04-00393), and Brain & Behavior Research Foundation Young and Independent Investigator Awards. A.Jam. [Oxford] was supported by Medical Research Council (MRC) grant G0500092. P.H. [SWIFT] is supported by a NARSAD grant from the Brain & Behavior Research Foundation (28445) and by a Research Grant from the Novartis Foundation (20A058). R.C.G. [UPENN] received funding through NIH grants 1R01MH117014 and 1R01MH119219. N.J. [ENIGMA] is funded by NIH grant R01MH117601. S.E.M. [ENIGMA] is supported in part by Australian NHMRC APP1172917. J.A.T. [FBIRN, MCIC, COBRE] is supported by NIH grant R01MH121246. Further acknowledgments specific to datasets are listed in the Supporting Information.

Competing interests

O.A.A. is a consultant to HealthLytix. J.B. has received royalties from UpToDate. D.H.M. is a consultant for Recognify Life Sciences Inc., and Syndesi Therapeutics. A.B. received consulting fees by Biogen and lecture fees by Otsuka, Janssen, and Lundbeck. C.M.D-C. has received honoraria from Exeltis and Angelini. C.Ar. has been a consultant to or has received honoraria or grants from Acadia, Angelini, Boehringer, Gedeon Richter, Janssen Cilag, Lundbeck, Minerva, Otsuka, Pfizer, Roche, Sage, Servier, Shire, Schering Plough, Sumitomo Dainippon Pharma, Sunovion and Takeda. S.K. receives royalties for cognitive test and training software from Schuhfried, Austria. B.F. has received educational speaking fees from Medice GmbH.

Author Contributions

D.S., M.C.P., S.E.F., B.F., D.C.G., R.C.G., R.H., N.J., E.L., S.E.M., P.M.T., J.A.T., T.G.M.vE., and C.F. designed the research; D.S., M.C.P., M.F., J.M., K.M., S.M.C.dZ., N.E.M.vH., W.C., H.E.HP., R.S.K., R.A-A, V.O-GdlF., D.T-G., J.V-B., B.C-F., D.A., A.D., L.T.W., I.A., O.A.A., E.G.J., P.K., J.M.B., S.V.C., P.T.M., B.J.M., Y.Q., P.E.R., U.S., R.J.S., V.J.C., M.J.G., F.A.H., C.M.L., C.P., C.S.W., T.W.W., L.dH., K.B., J-K.P., K.G.R., F.St., A.Jan., T.T.J.K., I.N., B.K., O.G., T.D.S., J.B., D.H.M., A.P., V.D.C., J.M.F., S.G.P., J.C., Y.T., Z.W., H.X., F.F., F.B., S.E., P.F-C., MA.G-L., A.G-P., R.S., S.S., E.P-C., V.C., F.P., D.V., N.B., G.S., S.M., T.vA., E.W.D., A.N.V., K.S., S.Ci., P.D.,

R.M.M., W-S.K., Y-C.C., C.An., A.Sc., S.B., A.M.McI., H.C.W., S.M.L., S.dP., H.K.L., F.Sc., R.E., D.G., R.L., U.D., J.T.E., K.R-M., J.M.S., A.R.M., L.A.A., L.F., G.P., A.B., C.M.D-C., J.J., N.G.L., C.Ar., A.S.T., I.L., S.Ce., C.M.S., F.G., M.Kir., S.K., T.H., A.Sk., F.Sp., M.Kim, YB.K., S.O., JS.K., A.Jam., G.B., C.K., M.S., V.O., A.U., F.M.H., D.J.S., H.S.T., A.M.D-Z., J.A.P-Z., C.L-J., S.H., E.J., W.S., P.H., D.C.G., R.C.G., R.H., J.A.T., and T.G.M.vE. acquired data and/or analyzed data and/or performed research; D.S. and C.F. wrote the paper; D.S., M.C.P., M.F., J.M., K.M., S.M.C.dZ., N.E.M.vH., W.C., H.E.HP., R.S.K., R.A-A, V.O-GdlF., D.T-G., J.V-B., B.C-F., D.A., A.D., L.T.W., I.A., O.A.A., E.G.J., P.K., J.M.B., S.V.C., P.T.M., B.J.M., Y.Q., P.E.R., U.S., R.J.S., V.J.C., M.J.G., F.A.H., C.M.L., C.P., C.S.W., T.W.W., L.dH., K.B., J-K.P., K.G.R., F.St., A.Jan., T.T.J.K., I.N., B.K., O.G., T.D.S., J.B., D.H.M., A.P., V.D.C., J.M.F., S.G.P., J.C., Y.T., Z.W., H.X., F.F., F.B., S.E., P.F-C., MA.G-L., A.G-P., R.S., S.S., E.P-C., V.C., F.P., D.V., N.B., G.S., S.M., T.vA., E.W.D., A.N.V., K.S., S.Ci., P.D., R.M.M., W-S.K., Y-C.C., C.An., A.Sc., S.B., A.M.McI., H.C.W., S.M.L., S.dP., H.K.L., F.Sc., R.E., D.G., R.L., U.D., J.T.E., K.R-M., J.M.S., A.R.M., L.A.A., L.F., G.P., A.B., C.M.D-C., J.J., N.G.L., C.Ar., A.S.T., I.L., S.Ce., C.M.S., F.G., M.Kir., S.K., T.H., A.Sk., F.Sp., M.Kim, YB.K., S.O., JS.K., A.Jam., G.B., C.K., M.S., V.O., A.U., F.M.H., D.J.S., H.S.T., A.M.D-Z., J.A.P-Z., C.L-J., S.H., E.J., W.S., P.H., S.E.F., B.F., D.C.G., R.C.G., R.H., N.J., E.L., S.E.M., P.M.T., J.A.T., T.G.M.vE., and C.F. critically reviewed the paper prior to submission.

Data availability

This study made use of 46 separate data sets collected around the world, under a variety of different consent procedures and regulatory bodies, during recent decades. Requests to access the data sets will be considered in relation to the relevant consents, rules and regulations, and can be made via the schizophrenia working group of the ENIGMA consortium: http://enigma.ini.usc.edu/ongoing/enigma-schizophrenia-working-group/.

References

1. American Psychiatric Association, Diagnostic and statistical manual of mental disorders, 5th edition, (American Psychiatric Association, 2013).
2. X.-Z. Kong *et al.*, Mapping cortical brain asymmetry in 17,141 healthy individuals worldwide via the ENIGMA Consortium. *Proc Natl Acad Sci U S A* **115**, E5154-E5163 (2018).
3. T. Guadalupe *et al.*, Human subcortical brain asymmetries in 15,847 people worldwide reveal effects of age and sex. *Brain Imaging Behav* **11**, 1497-1514 (2017).
4. V.R. Karolis, M. Corbetta, M. Thiebaut de Schotten, The architecture of functional lateralisation and its relationship to callosal connectivity in the human brain. *Nat Commun* **10**, 1417 (2019).
5. A.W. Toga, P.M. Thompson, Mapping brain asymmetry. *Nat Rev Neurosci* **4**, 37-48 (2003).
6. R.G. Petty, Structural asymmetries of the human brain and their disturbance in schizophrenia. *Schizophr Bull* **25**, 121-139 (1999).
7. M. Ribolsi, Z.J. Daskalakis, A. Siracusano, G. Koch, Abnormal asymmetry of brain connectivity in schizophrenia. *Front Hum Neurosci* **8**, 1010 (2014).
8. V. Oertel-Knöchel, D.E. Linden, Cerebral asymmetry in schizophrenia. *Neuroscientist* **17**, 456-467 (2011).
9. M.T. Berlim, B.S. Mattevi, P. Belmonte-de-Abreu, T.J. Crow, The etiology of schizophrenia and the origin of language: overview of a theory. *Compr Psychiatry* **44**, 7-14 (2003).
10. T.J. Crow, Schizophrenia as failure of hemispheric dominance for language. *Trends Neurosci* **20**, 339-343 (1997).
11. L.E. DeLisi *et al.*, Anomalous cerebral asymmetry and language processing in schizophrenia. *Schizophr Bull* **23**, 255-271 (1997).
12. S. Ocklenburg, O. Güntürkün, K. Hugdahl, M. Hirnstein, Laterality and mental disorders in the postgenomic age--A closer look at schizophrenia and language lateralization. *Neurosci Biobehav Rev* **59**, 100-110 (2015).
13. I. Sommer, N. Ramsey, R. Kahn, A. Aleman, A. Bouma, Handedness, language lateralisation and anatomical asymmetry in schizophrenia: meta-analysis. *Br J Psychiatry* **178**, 344-351 (2001).
14. K. Hugdahl *et al.*, Auditory verbal hallucinations in schizophrenia as aberrant lateralized speech perception: evidence from dichotic listening. *Schizophr Res* **140**, 59-64 (2012).
15. I.E. Sommer, N.F. Ramsey, R.S. Kahn, Language lateralization in schizophrenia, an fMRI study. *Schizophr Res* **52**, 57-67 (2001).
16. S. Ocklenburg, R. Westerhausen, M. Hirnstein, K. Hugdahl, Auditory hallucinations and reduced language lateralization in schizophrenia: a meta-analysis of dichotic listening studies. *J Int Neuropsychol Soc* **19**, 410-418 (2013).
17. J. Shapleske, S.L. Rossell, P.W. Woodruff, A.S. David, The planum temporale: a systematic, quantitative review of its structural, functional and clinical significance. *Brain Res Brain Res Rev* **29**, 26-49 (1999).
18. Y. Kawasaki *et al.*, Anomalous cerebral asymmetry in patients with schizophrenia demonstrated by voxel-based morphometry. *Biol Psychiatry* **63**, 793-800 (2008).
19. A. Hasan *et al.*, Planum temporale asymmetry to the right hemisphere in first-episode schizophrenia. *Psychiatry Res* **193**, 56-59 (2011).
20. J.N. de Boer *et al.*, Language in schizophrenia: relation with diagnosis, symptomatology and white matter tracts. *NPJ Schizophr* **6**, 10 (2020).
21. M. Hirnstein, K. Hugdahl, Excess of non-right-handedness in schizophrenia: meta-analysis of gender effects and potential biases in handedness assessment. *Br J Psychiatry* **205**, 260-267 (2014).
22. A. Deep-Soboslay *et al.*, Handedness, heritability, neurocognition and brain asymmetry in schizophrenia. *Brain* **133**, 3113-3122 (2010).
23. M. Dragovic, G. Hammond, Handedness in schizophrenia: a quantitative review of evidence. *Acta Psychiatr Scand* **111**, 410-419 (2005).
24. L.E. DeLisi *et al.*, Hand preference and hand skill in families with schizophrenia. *Laterality* **7**, 321-332 (2002).
25. K.G. Orr, M. Cannon, C.M. Gilvarry, P.B. Jones, R.M. Murray, Schizophrenic patients and their first-degree relatives show an excess of mixed-handedness. *Schizophr Res* **39**, 167-176 (1999).
26. A. Wiberg *et al.*, Handedness, language areas and neuropsychiatric diseases: insights from brain imaging and genetics. *Brain* **142**, 2938-2947 (2019).
27. G. Cuellar-Partida *et al.*, Genome-wide association study identifies 48 common genetic variants associated with handedness. *Nat Hum Behav* (2020).
28. Z. Sha *et al.*, The genetic architecture of structural left-right asymmetry of the human brain. *Nat Hum Behav* (2021).

29. Z. Sha, D. Schijven, C. Francks, Patterns of brain asymmetry associated with polygenic risks for autism and schizophrenia implicate language and executive functions but not brain masculinization. *Mol Psychiatry* (2021).
30. H.Y. Park *et al.*, Altered asymmetry of the anterior cingulate cortex in subjects at genetic high risk for psychosis. *Schizophr Res* **150**, 512-518 (2013).
31. X. Li *et al.*, Structural abnormalities in language circuits in genetic high-risk subjects and schizophrenia patients. *Psychiatry Res* **201**, 182-189 (2012).
32. M.E. Shenton, C.C. Dickey, M. Frumin, R.W. McCarley, A review of MRI findings in schizophrenia. *Schizophr Res* **49**, 1-52 (2001).
33. T.P. DeRamus *et al.*, Covarying structural alterations in laterality of the temporal lobe in schizophrenia: A case for source-based laterality. *NMR Biomed* **33**, e4294 (2020).
34. K.S.F. Damme, T. Vargas, V. Calhoun, J. Turner, V.A. Mittal, Global and Specific Cortical Volume Asymmetries in Individuals With Psychosis Risk Syndrome and Schizophrenia: A Mixed Cross-sectional and Longitudinal Perspective. *Schizophr Bull* **46**, 713-721 (2020).
35. J.F. Smiley *et al.*, Hemispheric asymmetry of primary auditory cortex and Heschl's gyrus in schizophrenia and nonpsychiatric brains. *Psychiatry Res* **214**, 435-443 (2013).
36. J. Sheng *et al.*, Altered volume and lateralization of language-related regions in first-episode schizophrenia. *Schizophr Res* **148**, 168-174 (2013).
37. K.S. Button *et al.*, Power failure: why small sample size undermines the reliability of neuroscience. *Nat Rev Neurosci* **14**, 365-376 (2013).
38. X.Z. Kong, C. Francks, Reproducibility in the absence of selective reporting: An illustration from large-scale brain asymmetry research. *Hum Brain Mapp* **43**, 244-254 (2022).
39. S. Marek *et al.*, Reproducible brain-wide association studies require thousands of individuals. *Nature* **603**, 654-660 (2022).
40. U. Ettinger *et al.*, Magnetic resonance imaging of the thalamus and adhesio interthalamica in twins with schizophrenia. *Arch Gen Psychiatry* **64**, 401-409 (2007).
41. J.G. Csernansky *et al.*, Abnormalities of thalamic volume and shape in schizophrenia. *Am J Psychiatry* **161**, 896-902 (2004).
42. H.B. Boos, A. Aleman, W. Cahn, H. Hulshoff Pol, R.S. Kahn, Brain volumes in relatives of patients with schizophrenia: a meta-analysis. *Arch Gen Psychiatry* **64**, 297-304 (2007).
43. N. Okada *et al.*, Abnormal asymmetries in subcortical brain volume in schizophrenia. *Mol Psychiatry* **21**, 1460-1466 (2016).
44. N. Okada *et al.*, Abnormal asymmetries in subcortical brain volume in early adolescents with subclinical psychotic experiences. *Transl Psychiatry* **8**, 254 (2018).
45. P.M. Thompson *et al.*, The ENIGMA Consortium: large-scale collaborative analyses of neuroimaging and genetic data. *Brain Imaging Behav* **8**, 153-182 (2014).
46. P.M. Thompson *et al.*, ENIGMA and the individual: Predicting factors that affect the brain in 35 countries worldwide. *Neuroimage* **145**, 389-408 (2017).
47. T.G.M. van Erp *et al.*, Cortical Brain Abnormalities in 4474 Individuals With Schizophrenia and 5098 Control Subjects via the Enhancing Neuro Imaging Genetics Through Meta Analysis (ENIGMA) Consortium. *Biol Psychiatry* **84**, 644-654 (2018).
48. T.G. van Erp *et al.*, Subcortical brain volume abnormalities in 2028 individuals with schizophrenia and 2540 healthy controls via the ENIGMA consortium. *Mol Psychiatry* **21**, 547-553 (2016).
49. X.Z. Kong *et al.*, Mapping brain asymmetry in health and disease through the ENIGMA consortium. *Hum Brain Mapp* -, 1-15 (2020).
50. C.G.F. de Kovel *et al.*, No Alterations of Brain Structural Asymmetry in Major Depressive Disorder: An ENIGMA Consortium Analysis. *Am J Psychiatry*, appiajp201918101144 (2019).
51. M.C. Postema *et al.*, Altered structural brain asymmetry in autism spectrum disorder in a study of 54 datasets. *Nat Commun* **10**, 4958 (2019).
52. X.Z. Kong *et al.*, Mapping Cortical and Subcortical Asymmetry in Obsessive-Compulsive Disorder: Findings From the ENIGMA Consortium. *Biol Psychiatry* (2019).
53. M.C. Postema *et al.*, Analysis of structural brain asymmetries in attention-deficit/hyperactivity disorder in 39 datasets. *J Child Psychol Psychiatry* (2021).
54. B.A. Gutman *et al.*, A meta-analysis of deep brain structural shape and asymmetry abnormalities in 2,833 individuals with schizophrenia compared with 3,929 healthy volunteers via the ENIGMA Consortium. *Hum Brain Mapp* (2021).
55. S. Malik-Moraleda *et al.*, An investigation across 45 languages and 12 language families reveals a universal language network. *Nat Neurosci* **25**, 1014-1019 (2022).

56. L. Labache *et al.*, A SENtence Supramodal Areas AtlaS (SENSAAS) based on multiple task-induced activation mapping and graph analysis of intrinsic connectivity in 144 healthy right-handers. *Brain Struct Funct* **224**, 859-882 (2019).
57. B. Fischl, FreeSurfer. *Neuroimage* **62**, 774-781 (2012).
58. R.S. Desikan *et al.*, An automated labeling system for subdividing the human cerebral cortex on MRI scans into gyral based regions of interest. *Neuroimage* **31**, 968-980 (2006).
59. B. Fischl *et al.*, Whole brain segmentation: automated labeling of neuroanatomical structures in the human brain. *Neuron* **33**, 341-355 (2002).
60. R Core Team, R: A language and environment for statistical computing. (2021).
61. Y.C. Lo *et al.*, The loss of asymmetry and reduced interhemispheric connectivity in adolescents with autism: a study using diffusion spectrum imaging tractography. *Psychiatry Res* **192**, 60-66 (2011).
62. D. Zhou, C. Lebel, A. Evans, C. Beaulieu, Cortical thickness asymmetry from childhood to older adulthood. *Neuroimage* **83**, 66-74 (2013).
63. S. Maingault, N. Tzourio-Mazoyer, B. Mazoyer, F. Crivello, Regional correlations between cortical thickness and surface area asymmetries: A surface-based morphometry study of 250 adults. *Neuropsychologia* **93**, 350-364 (2016).
64. B. Naimi, N.A.S. Hamm, T.A. Groen, A.K. Skidmore, A.G. Toxopeus, Where is positional uncertainty a problem for species distribution modelling? *Ecography* **37**, 191-203 (2014).
65. S. Nakagawa, I.C. Cuthill, Effect size, confidence interval and statistical significance: a practical guide for biologists. *Biol Rev Camb Philos Soc* **82**, 591-605 (2007).
66. W. Viechtbauer, Conducting Meta-Analyses in R with the metafor Package. *J Stat Softw* **36**, 48 (2010).
67. Y. Benjamini, Y. Hochberg, Controlling the False Discovery Rate: A Practical and Powerful Approach to Multiple Testing. *J R Stat Soc Series B Stat Methodol* **57**, 289-300 (1995).
68. M. Harrer, P. Cuijpers, T. Furukawa, D.D. Ebert, dmetar: Companion R Package For The Guide 'Doing Meta-Analysis in R'. (2019).
69. S.R. Kay, A. Fiszbein, L.A. Opler, The positive and negative syndrome scale (PANSS) for schizophrenia. *Schizophr Bull* **13**, 261-276 (1987).
70. N.C. Andreasen, The scale for the assessment of positive symptoms (SAPS), (The University of Iowa, 1984).
71. N.C. Andreasen, The scale for the assessment of negative symptoms (SANS), (The University of Iowa, 1984).
72. S. Kim, ppcor: An R Package for a Fast Calculation to Semi-partial Correlation Coefficients. *Commun Stat Appl Methods* **22**, 665-674 (2015).
73. J. Radua *et al.*, Increased power by harmonizing structural MRI site differences with the ComBat batch adjustment method in ENIGMA. *Neuroimage* **218**, 116956 (2020).
74. S.S. Sawilowsky, New effect size rules of thumb. *J Mod Appl Stat Methods* **8**, 26 (2009).
75. C. Francks, Exploring human brain lateralization with molecular genetics and genomics. *Ann N Y Acad Sci* **1359**, 1-13 (2015).
76. G. Vingerhoets, Phenotypes in hemispheric functional segregation? Perspectives and challenges. *Phys Life Rev* **30**, 1-18 (2019).
77. J. Schmitz *et al.*, Hemispheric asymmetries in cortical gray matter microstructure identified by neurite orientation dispersion and density imaging. *Neuroimage* **189**, 667-675 (2019).
78. V.S. Natu *et al.*, Apparent thinning of human visual cortex during childhood is associated with myelination. *Proc Natl Acad Sci U S A* **116**, 20750-20759 (2019).
79. M.F. Glasser, D.C. Van Essen, Mapping human cortical areas in vivo based on myelin content as revealed by T1- and T2-weighted MRI. *J Neurosci* **31**, 11597-11616 (2011).
80. Y. Cui *et al.*, Auditory verbal hallucinations are related to cortical thinning in the left middle temporal gyrus of patients with schizophrenia. *Psychol Med* **48**, 115-122 (2018).
81. E. Sprooten *et al.*, Cortical thickness in first-episode schizophrenia patients and individuals at high familial risk: a cross-sectional comparison. *Schizophr Res* **151**, 259-264 (2013).
82. M. Hu *et al.*, Decreased left middle temporal gyrus volume in antipsychotic drug-naive, first-episode schizophrenia patients and their healthy unaffected siblings. *Schizophr Res* **144**, 37-42 (2013).
83. A.E. Cullen *et al.*, Temporal lobe volume abnormalities precede the prodrome: a study of children presenting antecedents of schizophrenia. *Schizophr Bull* **39**, 1318-1327 (2013).
84. M.S. Panizzon *et al.*, Distinct genetic influences on cortical surface area and cortical thickness. *Cereb Cortex* **19**, 2728-2735 (2009).
85. K.L. Grasby *et al.*, The genetic architecture of the human cerebral cortex. *Science* **367** (2020).
86. W. Tang *et al.*, A connectional hub in the rostral anterior cingulate cortex links areas of emotion and cognitive control. *Elife* **8** (2019).

87. T.S. Bhojraj *et al.*, Gray matter loss in young relatives at risk for schizophrenia: relation with prodromal psychopathology. *Neuroimage* **54 Suppl 1**, S272-279 (2011).
88. H. He *et al.*, Altered asymmetries of diffusion and volumetry in basal ganglia of schizophrenia. *Brain Imaging Behav* **15**, 782-787 (2021).
89. M.K. Dougherty *et al.*, Differences in subcortical structures in young adolescents at familial risk for schizophrenia: a preliminary study. *Psychiatry Res* **204**, 68-74 (2012).
90. K.S. Smith, A.J. Tindell, J.W. Aldridge, K.C. Berridge, Ventral pallidum roles in reward and motivation. *Behav Brain Res* **196**, 155-167 (2009).
91. S. Galderisi, A. Mucci, R.W. Buchanan, C. Arango, Negative symptoms of schizophrenia: new developments and unanswered research questions. *Lancet Psychiatry* **5**, 664-677 (2018).
92. C.G.F. de Kovel *et al.*, Left-Right Asymmetry of Maturation Rates in Human Embryonic Neural Development. *Biol Psychiatry* **82**, 204-212 (2017).
93. P.G. Hepper, S. Shahidullah, R. White, Handedness in the human fetus. *Neuropsychologia* **29**, 1107-1111 (1991).
94. R. Hering-Hanit, R. Achiron, S. Lipitz, A. Achiron, Asymmetry of fetal cerebral hemispheres: in utero ultrasound study. *Arch Dis Child Fetal Neonatal Ed* **85**, F194-196 (2001).
95. P.G. Hepper, D.L. Wells, C. Lynch, Prenatal thumb sucking is related to postnatal handedness. *Neuropsychologia* **43**, 313-315 (2005).
96. C. Chiron *et al.*, The right brain hemisphere is dominant in human infants. *Brain* **120 (Pt 6)**, 1057-1065 (1997).
97. J.J. Joyce *et al.*, Normal right and left ventricular mass development during early infancy. *Am J Cardiol* **93**, 797-801 (2004).
98. Z. Sha *et al.*, Handedness and its genetic influences are associated with structural asymmetries of the cerebral cortex in 31,864 individuals. *Proc Natl Acad Sci U S A* **118** (2021).
99. J.M. Roe *et al.*, Asymmetric thinning of the cerebral cortex across the adult lifespan is accelerated in Alzheimer's disease. *Nat Commun* **12**, 721 (2021).
100. A. Mundorf, J. Peterburs, S. Ocklenburg, Asymmetry in the Central Nervous System: A Clinical Neuroscience Perspective. *Front Syst Neurosci* **15**, 733898 (2021).
101. D. Koshiyama *et al.*, Neuroimaging studies within Cognitive Genetics Collaborative Research Organization aiming to replicate and extend works of ENIGMA. *Hum Brain Mapp* (2020).
102. D.N. Greve *et al.*, A surface-based analysis of language lateralization and cortical asymmetry. *J Cogn Neurosci* **25**, 1477-1492 (2013).
103. J. Lv *et al.*, Individual deviations from normative models of brain structure in a large cross-sectional schizophrenia cohort. *Mol Psychiatry* (2020).
104. Z. Liu *et al.*, Resolving heterogeneity in schizophrenia through a novel systems approach to brain structure: individualized structural covariance network analysis. *Mol Psychiatry* (2021).
105. H. Wickham, ggplot2: Elegant Graphics for Data Analysis, (Springer-Verlag New York, 2016).
106. A. South, rnaturalearth: World Map Data from Natural Earth. R package version 0.1.0. https://CRAN.R-project.org/package=rnaturalearth. (2017).
107. E. Pebesma, Simple Features for R: Standardized Support for Spatial Vector Data. *R J* **10**, 439-446 (2018).
108. K. Slowikowski, ggrepel: Automatically Position Non-Overlapping Text Labels with 'ggplot2'. R package version 0.9.1. https://CRAN.R-project.org/package=ggrepel. (2021).

Figures and tables

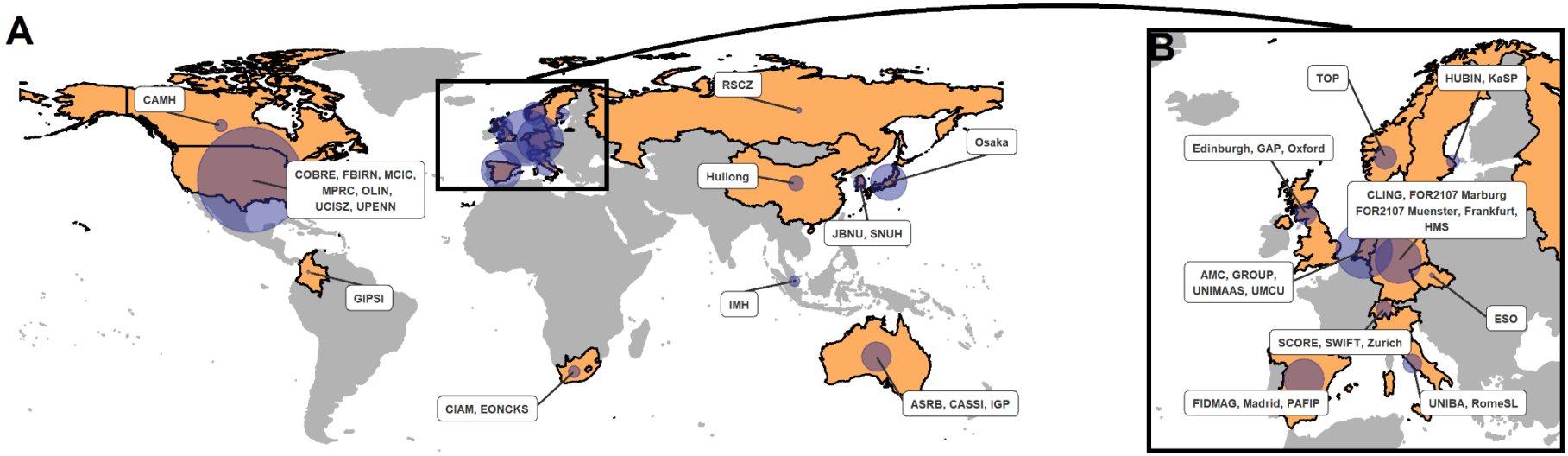

Figure 1. Geographic origin of included datasets. A) Countries from which one or more datasets originate are highlighted in the world map, with dataset names included in labels. The relative sample size of datasets per country is indicated by blue circles. **B)** Zoomed map of Europe. For more details, see Table 1. Figure generated in R using packages *ggplot2* (105), *rnaturalearth* (106), *sf* (107) and *ggrepel* (108).

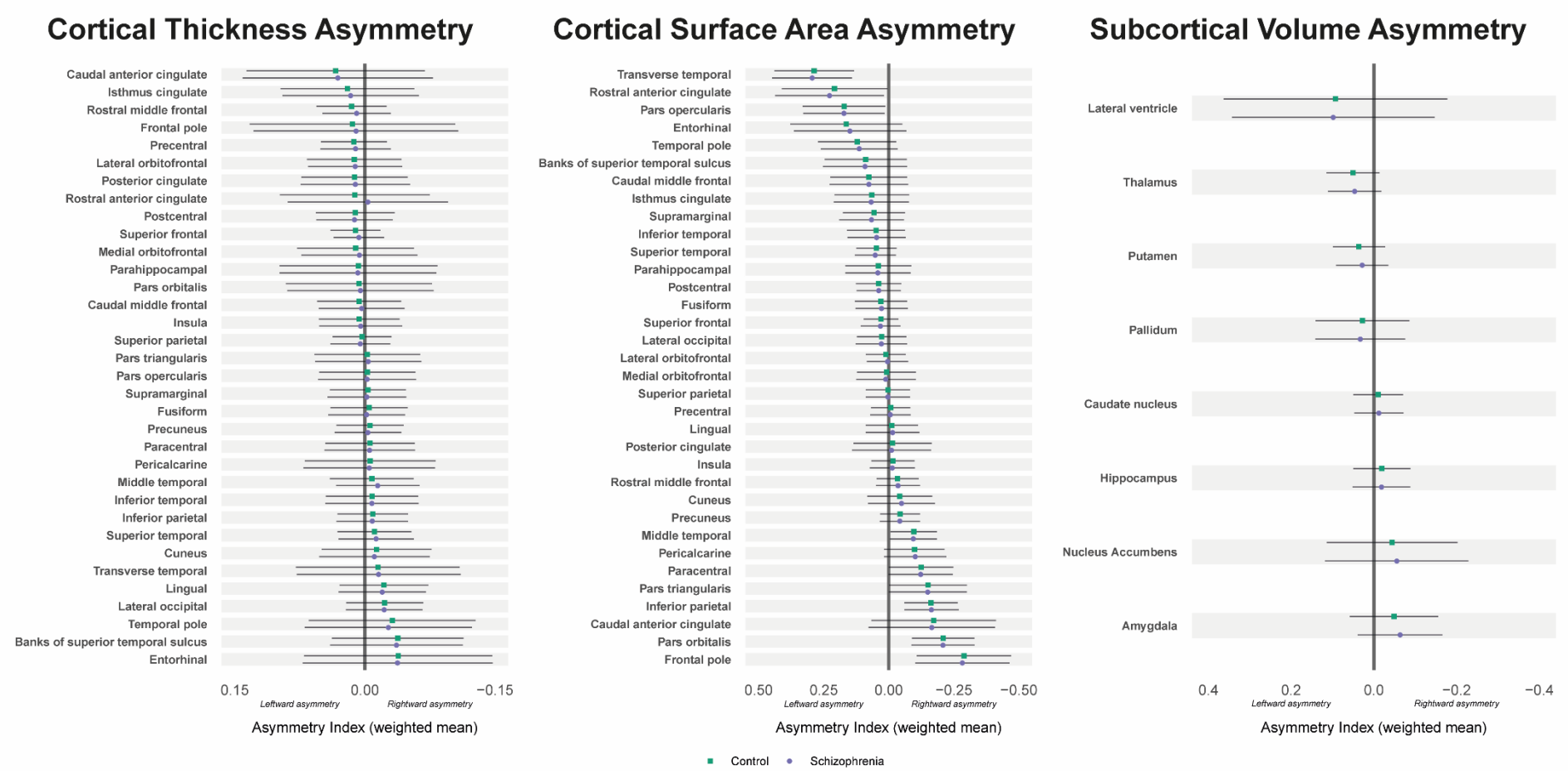

Figure 2. Average structural asymmetries of the brain in individuals with schizophrenia and unaffected controls. For each bilaterally paired structural measure, the mean asymmetry index (AI) across datasets, weighted by sample size, is shown for individuals with schizophrenia (purple) and unaffected controls (green). A positive AI indicates left > right asymmetry, whereas a negative AI indicates right > left asymmetry. Error bars show pooled standard deviations. Figure generated in R using package *ggplot2* (105).

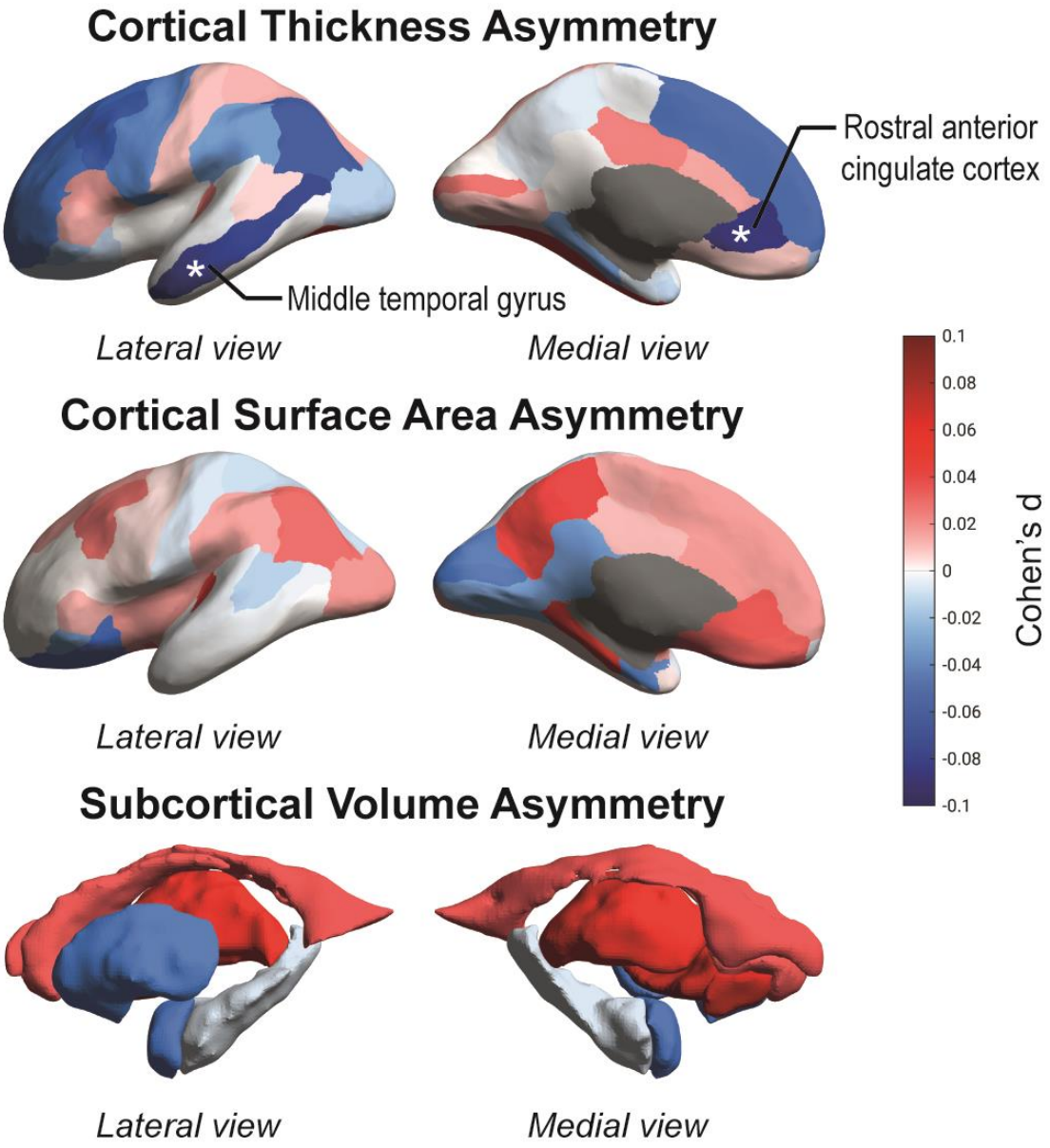

Figure 3. Map of cortical and subcortical asymmetry differences between individuals with schizophrenia and unaffected controls. Cohen's *d* effect sizes from random-effects meta-analysis are projected on inflated left hemisphere cortical surface models (for cortical thickness and surface area) or subcortical structures (for subcortical volumes). Positive effects are shown in red shades (larger leftward or smaller rightward asymmetry in cases versus controls), while negative effects are shown in blue shades (smaller leftward or larger rightward asymmetry in cases versus controls). Gray shades indicate masked out structures. See also Fig. 2 and Table S4 for directions of effects. Regions significant at $p_{FDR} < 0.05$ are labelled and marked with asterisks.

Table 1. Overview of the ENIGMA-Schizophrenia datasets.

			Individuals with schizophrenia		Unaffected Controls	
Dataset	**Country**	**N Total**	**N M/F**	**Mean age (years)**	**N M/F**	**Mean age (years)**
AMC	Netherlands	405	180 / 26	22.2	130 / 69	23.5
ASRB*	Australia	429	177 / 86	38.6	79 / 87	39.3
CAMH	Canada	264	70 / 48	44.0	77 / 69	43.6
CASSI*	Australia	116	35 / 18	35.2	33 / 30	30.5
CIAM	South Africa	51	13 / 8	31.1	16 / 14	26.6
CLING	Germany	371	35 / 13	32.4	132 / 191	25.2
COBRE*	United States	143	60 / 13	37.4	50 / 20	35.7
EdinburghEHRS	United Kingdom	67	19 / 12	21.8	17 / 19	21.2
EdinburghFunc	United Kingdom	60	11 / 14	37.2	18 / 17	37.5
EdinburghSFMH	United Kingdom	76	23 / 12	37.5	23 / 18	38.2
EONCKS*	South Africa	200	74 / 34	34.2	51 / 41	31.9
ESO*	Czech Republic	80	20 / 20	29.5	20 / 20	29.1
FBIRN	United States	359	139 / 46	39.0	124 / 50	37.5
FIDMAG	Spain	283	124 / 36	39.6	54 / 69	37.5
FOR2107 Marburg*	Germany	403	23 / 14	37.2	143 / 223	34.0
FOR2107 Muenster*	Germany	163	4 / 4	33.4	60 / 95	27.0
Frankfurt	Germany	59	20 / 9	38.1	13 / 17	35.2
GAP	United Kingdom	209	85 / 37	27.5	32 / 55	25.9
GIPSI	Colombia	43	35 / 8	33.5	-	-
GROUP	Netherlands	271	59 / 29	28.2	83 / 100	30.1
HMS	Germany	101	32 / 14	28.4	28 / 27	35.4
HUBIN	Sweden	196	70 / 24	41.7	69 / 33	42.0
Huilong	China	333	133 / 112	25.5	49 / 39	27.7
IGP*	Australia	138	40 / 28	41.7	38 / 32	36.0
IMH*	Singapore	227	105 / 46	33.1	47 / 29	31.8
JBNU	South Korea	208	57 / 37	39.3	48 / 66	41.4
KaSP	Sweden	88	34 / 22	30.3	15 / 17	27.5
Madrid	Spain	105	17 / 4	16.2	59 / 25	11.8
MCIC	United States	311	113 / 35	32.9	101 / 62	31.4
MPRC*	United States	437	128 / 78	35.4	96 / 135	37.1
OLIN*	United States	868	174 / 138	37.7	310 / 246	37.6
Osaka	Japan	855	118 / 98	36.1	318 / 321	34.1
Oxford	United Kingdom	74	24 / 17	16.3	15 / 18	16.1
PAFIP	Spain	556	214 / 138	29.9	127 / 77	29.2
RomeSL	Italy	280	110 / 54	39.4	73 / 43	37.5
RSCZ	Russia	98	46 / 0	22.2	52 / 0	22.3
SCORE	Switzerland	205	117 / 44	25.5	17 / 27	25.5
SNUH	South Korea	80	18 / 22	22.9	20 / 20	22.6
SWIFT	Switzerland	37	17 / 7	34.2	5 / 8	29.3
TOP	Norway	522	130 / 89	32.0	159 / 144	35.4
UCISZ*	United States	57	22 / 5	42.9	23 / 7	41.4
UMCU	Netherlands	600	236 / 79	30.9	165 / 120	32.9
UNIBA*	Italy	143	54 / 19	33.5	28 / 42	26.6
UNIMAAS	Netherlands	66	21 / 10	28.3	24 / 11	28.1
UPENN	United States	370	105 / 72	38.9	90 / 103	36.4
Zurich*	Switzerland	88	45 / 15	30.5	18 / 10	32.5
Total/Mean		11,095	3,386 / 1,694	33.3	3,149 / 2,866	33.0

All datasets are shown with their total sample sizes and the numbers of male (M) and female (F) individuals with and without schizophrenia, as well as mean ages. For datasets marked with *, we had access to the individual-level data for the multivariate analysis. Exact sample sizes in the multivariate analysis are shown in Table S1C.

Table 2. Significant brain regional asymmetry differences between individuals with schizophrenia and unaffected controls.

	Sample size (N)		Mean AI (SD)		Cohen's d effect size [95% CI]			Average asymmetry	
Structural AI	**Control**	**Schizophrenia**	**Control**	**Schizophrenia**	**Left**	**Right**	**AI**	**Control**	**Schizophrenia**
Rostral anterior cingulate cortex (cortical thickness asymmetry)	5,811	4,851	0.012 (0.086)	-0.0035 (0.092)	-0.20 [-0.28, -0.11]	-0.094 [-0.15, -0.036]	-0.083 [-0.13, -0.032]	Leftward	Reversed to rightward
Middle temporal gyrus (cortical thickness asymmetry)	5,673	4,684	-0.0080 (0.048)	-0.015 (0.048)	-0.41 [-0.50, -0.32]	-0.36 [-0.44, -0.27]	-0.074 [-0.12, -0.026]	Rightward	Increased rightward

Mean AI = weighted mean asymmetry index across datasets. SD = pooled standard deviation across datasets (positive mean indicates average leftward asymmetry; negative mean indicates average rightward asymmetry). Cohen's *d* effect sizes are shown from separate meta-analysis of left-hemisphere, right-hemisphere and asymmetry index differences between cases and controls. No regional measures of cortical surface area asymmetry or subcortical volume asymmetry showed significant case-control differences after false discovery rate correction.

Table 3. Multivariate analysis of case-control brain asymmetry differences between 935 individuals with schizophrenia and 1,094 controls for which individual-level data were available (14 datasets).

Structural asymmetry	***Approximate F***	***p***
Multivariate test (all regional cortical and subcortical asymmetries)	1.87	Nominal $p = 1.25 \times 10^{-5}$ Permutation $p = 3.0 \times 10^{-6}$

Most significant univariate effects:	***F***	***p***
Pallidum (volume asymmetry)	29.1	7.8×10^{-8}
Nucleus accumbens (volume asymmetry)	9.3	2.3×10^{-3}
Rostral middle frontal gyrus (surface area asymmetry)	7.7	5.5×10^{-3}
Parahippocampal gyrus (surface area asymmetry)	7.2	7.4×10^{-3}
Parahippocampal gyrus (thickness asymmetry)	5.5	0.019
Transverse temporal gyrus (thickness asymmetry)	5.4	0.021
Cuneus (surface area asymmetry)	5.4	0.021
Banks of superior temporal sulcus (surface area asymmetry)	4.9	0.027
Insula (surface area asymmetry)	4.6	0.031
Medial orbitofrontal cortex (thickness asymmetry)	3.9	0.048

Results are shown for the multivariate MANCOVA over all asymmetries, and the specific asymmetries with nominal significance ($p < 0.05$) in the corresponding univariate ANCOVAs, with their F statistics (*F*) and p-values (*p*).